

# PRINTED HUMIDITY SENSOR FOR PACKAGING



**Prifysgol Abertawe  
Swansea University**

**Modem Abiram Reddy**

A Dissertation Submitted to the Swansea University in fulfilment of the requirements for the Degree Mechanical Engineering through Research in the Department of Welsh Centre for Printing and Coating  
Swansea University

June 2022



**Declarations**

This work has not previously been accepted in substance for any degree and is not being concurrently submitted in candidature for any degree.

Signed.



Date ..... 16-06-2022 .....

This thesis is the result of my own investigations, except where otherwise stated. Other sources are acknowledged by footnotes giving explicit references. A bibliography is appended.

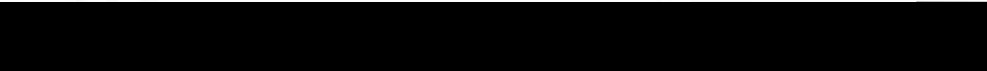
Signed



Date ..... 16-06-2022 .....

I hereby give consent for my thesis, if accepted, to be available for photocopying and for inter-library loan, and for the title and summary to be made available to outside organisations.

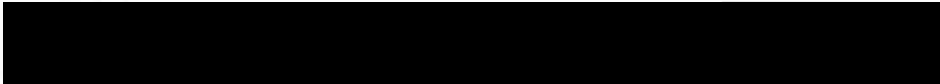
Signed.



Date ..... 16-06-2022 .....

The University's ethical procedures have been followed and, where appropriate, that ethical approval has been granted.

Signe



Date ..... 16-06-2022 .....

## Acknowledgements

Throughout the writing of this dissertation I have received a great deal of assistance and support. I would first like to thank my supervisor Prof Tim Claypole for all the invaluable expertise throughout my research and methodology.

I would particularly like to single out my other main mentor Dr. John Lau for all the excellent co-operation and support given to me in the lab and the added knowledge in this field during my period of study. I would like to acknowledge my fellow colleague's Dr Ben Clifford, Dr Alex Holder, Dr Sakulrat Foulston and Ms Caitlin McCall for their valuable guidance and providing me with the right tools that I needed to successfully complete my dissertation.

In addition to this, I would like to thank my parents and friends who were of great support during the course as well as providing me happy distraction to rest my mind outside my research.

## Abstract

Printed electronics is the process of developing electrical devices on different substrates by printing inks by various methods. Flexographic printing a Humidity sensor was investigated. Flexographic printing can be cost effective for volume production on label presses. In this research, conductive silver nano-particle ink with a Silver content of 50 (+/-2) Wt.% was used to develop an Interdigitated Electrode (IDE). The printed base Silver interdigitated electrodes had an average resistance of  $11.96\Omega$  with a standard deviation of 1.21 indicating that the Silver printed sensors were consistent in the print quality.

Nafion (a sulfonated tetrafluoroethylene-based copolymer) resin solution with a 20 wt.% in lower aliphatic alcohols and water, was printed on top of the silver Interdigitated electrode as the active layer for the detection of the change in humidity. Substrate used for the experiment was white Polyethylene terephthalate (PET White) of 0.175mm thickness. The sensors were tested in a Humidity chamber over a range of 40-80% relative humidity at of  $25^{\circ}\text{C}$  to ascertain the effective working of the design by measuring their resistivity and repeatability. When the resistance of the sensors was checked with Direct Current (DC), there was a change in the resistance. The formation of dendrites due to electro-chemical reactivity on the surface of the sensor was observed, which caused the sensors to short circuit and fail. When the sensors were tested with Alternating Current (AC), it limited the growth of dendrites and the sensors were self-consistent with a repeatability of resistance pattern, but there was variation in the range of resistance between the sensors, where few showed sensing activity that started at around  $500\text{ K}\Omega$  and others around  $2000\text{ K}\Omega$  at 40%RH (Relative Humidity). This proved that the materials used worked and showed potential in developing a humidity sensor via Flexographic printing, further worked is required to eliminate the Dendrites formation and to stabilize the range of resistance.

# Contents

<b>List of Figures</b>	VIII
<b>List of Tables</b>	X
<b>1 Introduction</b>	<b>1</b>
<b>2 Literature Survey</b>	<b>2</b>
2.1 Electrodes and Interdigitated Electrodes . . . . .	2
2.2 Printed Electronics . . . . .	3
2.3 Flexography . . . . .	4
2.4 Screen Printing . . . . .	6
2.5 Surface Energy and Dyne Level . . . . .	7
2.6 Conductive Inks and Substrates . . . . .	8
2.7 Active layer Inks . . . . .	11
2.8 Summary . . . . .	17
<b>3 Methodology</b>	<b>18</b>
3.1 Equipment used in the study . . . . .	18
3.1.1 RK Flexiproofer . . . . .	18
3.1.2 Anilox Roll . . . . .	19
3.1.3 3D Microscopy Alicona . . . . .	20
3.1.4 Wyko Veeco Surface Profiler . . . . .	22
3.1.5 Kinexus Pro Plus Rheometer . . . . .	24
3.2 Materials . . . . .	26
3.2.1 Substrates . . . . .	26
3.2.2 Cyan Ink . . . . .	27
3.2.3 Conductive Inks . . . . .	27
3.2.4 Active Material . . . . .	28
3.2.5 Printing Plates . . . . .	30
3.2.6 Interdigitated Electrode Structure and Plate Design . . . . .	31
<b>4 Printing Interdigitated Electrodes</b>	<b>33</b>
4.1 Introduction . . . . .	33
4.2 Optimization of print settings using process cyan ink . . . . .	34
4.3 Print Quality of Silver . . . . .	37

4.4	Profiling of Printed Silver IDE . . . . .	38
4.5	Silver Print Setup Analysis . . . . .	40
4.6	Electrical Resistance of the Printed Silver IDEs . . . . .	44
<b>5</b>	<b>Humidity Chamber Testing</b>	<b>46</b>
5.1	Humidity Chamber Setup . . . . .	46
5.2	Direct Current measurement . . . . .	47
5.3	Dendritic Growth . . . . .	50
5.4	Alternating Current measurement . . . . .	52
5.5	Discussion . . . . .	54
<b>6</b>	<b>Conclusion and Futurework</b>	<b>56</b>
	<b>References</b>	<b>58</b>

## List of Abbreviations

AC	Alternating Current
Au	Gold
Ag NW	Silver Nanowires
BOPP	Biaxially oriented Polypropylene
CCD	Charge-coupled Device
CPP	Cast un-oriented Polypropylene
cm <sup>3</sup>	Centimetre per cube
DC	Direct Current
EIS	Electrochemical impedance spectroscopy
G.O	Graphene Oxide
ICP	Intrinsically Conducting Polymers
IDE	Interdigitated Electrode
Kg/cm <sup>2</sup>	Kilogram per centimetre squared
kHz	Kilo Hertz
LCR	Inductance-Capacitance-Resistance
LOC	Lab-on-chip
m <sup>2</sup>	Metre square
mm	Millimetre
m/min	Metre per min
N/cm	Newton per centimetre
Nm	Nano metre
Pa.s	Pascal per second
PET	Polyethylene Terephthalate
PEDOT	Poly(3,4-ethylenedioxythiophene)
PP	Polypropylene
PS	Poly (styrene sulfonate)
rH/RH	Relative Humidity
SnO <sub>2</sub>	Tin Peroxide
TiO <sub>2</sub>	Titanium Peroxide
UV	Ultraviolet
V	Volts
WLI	White light Interferometry
Wt.%	Weight percent
ZnO	Zinc Peroxide
3D	3-Dimensional
°C	Degree centigrade
Ω	Ohms
KΩ	Kilo Ohms
μm	Micro metre



## List of Figures

1	Printed Silver Interdigitated Electrodes . . . . .	3
2	Flexography Printing . . . . .	5
3	Screen Printing Technology . . . . .	6
4	Surface Energy . . . . .	7
5	Time and Humidity Resistance Graph [13] . . . . .	8
6	Lateral Sensor Array [14] . . . . .	9
7	Time Response [14] . . . . .	9
8	Aerosol jet deposition device structure [15] . . . . .	10
9	Fabrication process of Au and Nafion based Sensor [18] . . . . .	11
10	Repetability Characteristics of the sensor [15] . . . . .	12
11	Adsorption and Desorption of Nafion/Titanium oxide sensor [16] . . . . .	12
12	Ag NWs and Nafion Membrane Based Humidity Sensor [21] . . . . .	13
13	Electrical response mechanism of the Nafion/Ag NWs [21] . . . . .	13
14	Nafion capacitance versus time at 1, 10 and 100 kHz [18] . . . . .	14
15	Adsorption and Desorption of Iron oxide based sensor [25] . . . . .	15
16	Graphene Oxide based Humidity Sensor [17] . . . . .	15
17	Results of G.O sensor compared to commercial sensor [17] . . . . .	16
18	Flexiproofer . . . . .	18
19	$8\text{cm}^3/\text{m}^2$ Anilox . . . . .	19
20	$8\text{cm}^3/\text{m}^2$ Anilox Closeup . . . . .	19
21	Alicona . . . . .	20
22	Optical 3D measurement schematics [49] . . . . .	21
23	Whitelight interferometry schematics . . . . .	22
24	Wyko Veeco NT Series . . . . .	23
25	Gap Test . . . . .	25
26	Viscosity vs Time . . . . .	25
27	Nafion Perfluorinated Resin Structure . . . . .	29
28	IDE structure [Track Width: $300\mu\text{m}$ ][Gap: $500\mu\text{m}$ ] . . . . .	31
29	Base Layer Plate Design [Track Width: $300\mu\text{m}$ ] . . . . .	32
30	Top Layer Plate Design . . . . .	32
31	Sensor Structure . . . . .	33
32	Cyan print with patches when using insufficient engagement . . . . .	34
33	Cyan Print with excess Ink . . . . .	35

34	Good cyan print . . . . .	36
35	Good silver IDEs examples . . . . .	37
36	Example representation of selecting random regions . . . . .	39
37	Example of an IDE set . . . . .	40
38	IDEs Fingers Merging [Track Width:400 $\mu m$ , Gap:100 $\mu m$ ] . . . . .	40
39	Scatter Plot Representing printed silver height and widths of different IDEs .	41
40	Average height and width of 200 $\mu m$ IDEs . . . . .	43
41	2 Wire Method . . . . .	44
42	Average Silver IDE Resistance . . . . .	45
43	Relative humidity testing setup . . . . .	46
44	Electrical Resistance of 400 $\mu m$ width nafion coated IDEs . . . . .	48
45	Dendrite formation . . . . .	49
46	Dendrite observed via microscope . . . . .	51
47	200 $\mu m$ width IDE resistance tested using AC . . . . .	52
48	Range of resistance when tested with AC . . . . .	53

## List of Tables

1	Substrate . . . . .	26
2	PFI-500 . . . . .	27
3	Nafion Specification . . . . .	29
4	Printing Plate . . . . .	30
5	IDE Width on Plate Design vs Actual . . . . .	30
6	Flexiproofer Settings . . . . .	37
7	Mean Electrical Resistance of IDEs . . . . .	45
8	Alternating Current Test Settings . . . . .	54

# 1 Introduction

Humidity is a measurement of the amount of water present in the atmosphere, which can be a mixture like air or pure gas [1]. Relative Humidity (RH) is a measure of humidity. Colorimetric sensors were used to detect gas or record the change in temperature/humidity have been developed by stacking 2 or more chemical compound layer [2]. As further developments were made, the research shifted towards an approach which was more cost effective and could be produced on a larger scale at a faster pace. This was made possible by creating small conductive electrode structures. Using this as a base, different types of active layers could be coated on top for a variety of uses.

Traditionally printing any material using process such as Gravure, Screen Printing, Offset and Flexography relied on the skill of the operator using trial and error to find the correct settings to be applied for the desired output to be achieved. New intricate machines are developed every year for converting which reduce the time required for the product to be manufactured. This opens a wide scope for producing functional products which were not previously possible or very difficult to manufacture. Various functional products are being invented and manufactured on a large scale for the betterment and convenience of daily life of the end consumer.

There is a scope for developing a wide array of sensors using these printing technologies on a large scale and at a relatively low production cost. Sensors which can detect change in their surroundings are widely used, such as gas sensors, pressure sensors, radiation sensors, temperature and humidity sensors. They are vital when it comes to recording or detecting changes where monitoring ambience is crucial and can also be a safety feature. As the development of medicines grows and there is an increase in transportation of these medicines around the globe, the humidity sensor, the topic of research in this thesis, should be able to monitor sensitive medicines with respect to their advised normal temperature and humidity in applications such as transporting vaccines [3], which if they are exceeded cannot be administered.

This research looks at the feasibility and challenges faced while developing a humidity sensor via flexographic printing. There are many different factors that fall into play when manufacturing these sensors, such as substrate, inks, active materials, and testing.

## 2 Literature Survey

Developing a humidity sensing self-adhesive device of the size of a coin would be very useful in a commercial scenario. Manufacturing these devices in large scale production, can be achieved by implementing high volume in-line Flexographic printing. The proposed research was about developing this device via Flexographic technique using conductive inks and active materials.

Multiple papers have been researched on developing a Humidity sensor, where the main emphasis is on the following questions:

- Common materials used among the developed sensors and their differences
- The relationship between the ink and the active layer and their reactions.
- What is the most common method of developing the sensor and it's disadvantages.

### 2.1 Electrodes and Interdigitated Electrodes

A basic definition of electrode by Grimnes, et al [4], is a device which is a good conductor of electricity and usually connected to non-metallic parts of a circuit. There are two main types of electrodes which are reactive and inert electrodes. An inert electrode is not involved in any reaction while the reactive ones are. Gold, Carbon and Platinum are classified as inert electrodes, whereas Copper, Zinc, Silver are reactive electrodes. The use of an electrode is to carry the electric current and send it through non-metal object to alter them in different ways.

Interdigitated Electrodes (IDEs) as described by Rivadeneyra, et al [5], are the most widely used transducers which are made of two interdigitated comb electrode. This is used to increase the effective capacitance of the structure and increase the effective active area of the sensor. These also help to confine the electric field more effectively in active polymer layers that are coated on top of it. Interdigitated electrodes are used in the field of Biological, Chemical and Medical industries as sensors, due to their cost-effective production and extreme sensitivity.

## 2.2 Printed Electronics

Printed electronics refers to the printing of electronic circuits or devices on a range of substrates, [6]. These are being used to create lightweight keyboards, antennas, and electronic skin patches as the market for wearable devices and thinner electronics grows. Printing machines can print electrical circuits at a low cost and in a short amount of time. Printed electronics is one of the most rapidly evolving innovations, with applications in healthcare, aerospace, media, and transportation.

Silver inks is one of the conductive inks used to print electrical circuits as explained by Kamyshny, et al [7]. Silver inks are being adapted for printing conductive mass-producing conductive circuits, by flexography, can be cost-efficient and time saving. There are challenges to overcome to standardize printing of the sensors as they are sensitive materials and need to be handled carefully unlike graphics inks to avoid unwanted results. Figure 1 shows an example of a Silver Interdigitated Electrode developed in this research.

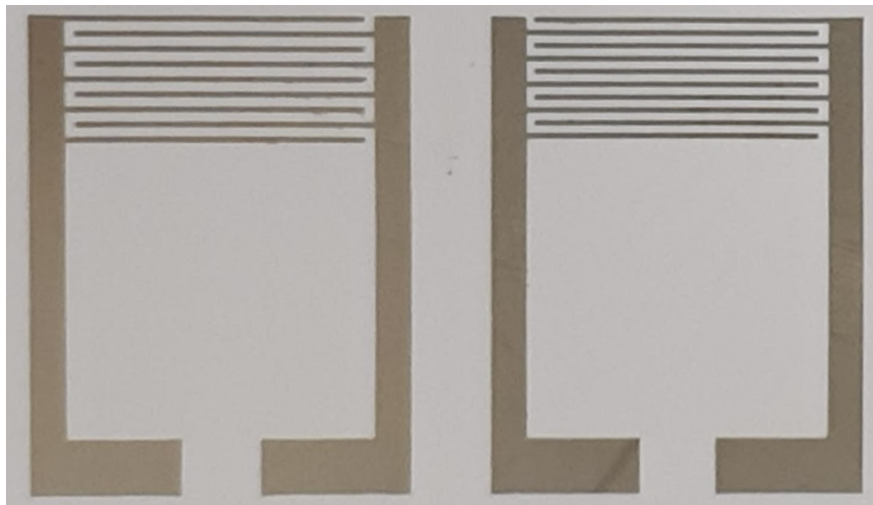


Figure 1: Printed Silver Interdigitated Electrodes

## 2.3 Flexography

The high speed printing process used for most label and packaging is Flexography which is a roll to roll process as explained by Joanna, et al [8]. Each station has generally an individual plate for each different colour of the image. Additional features include die cutting, lamination or embossing. Flexographic printing results in the process of producing labels which can be cost effective, fast throughput and of high quality. Multiple types of substrates can be used such as:

- Cardboard
- Plastic films
- Paper
- Metallic surfaces

Application of this process leads to the manufacturing of finished goods that would come in direct contact with consumer end products such as self adhesive labels for pharmaceutical companies or food packaging. This process is also used to manufacture high-end sensors for applications such as in industrial environment to detect toxic or in packaging to track and trace products. Important components of a flexographic machine are shown in figure 2.

- **Fountain Roller** This is in contact with the ink tray and the anilox roller. It picks up the ink and transfers it to the anilox roller.
- **Anilox roller** This roller has finely engraved cells measured in terms of Billion Cubic Microns that meters the ink transfer onto to the printing plate, Claypole, et al [9]. Different anilox have different cell depths. The volume of anilox selected for a print is dependent on the type of image being printed. Image with fine details require smaller volume anilox, where are solid block images require higher volume anilox. Doctor blade removes excess ink from the non-engraved part of the anilox.

- **Plate Cylinder** This holds the flexible printing plate used to print, using double sided tape. Different stiffness of tapes allows minute variation of impression of the image from the plate to the substrate.
- **Impression Cylinder** This applies pressure on to the substrate along plate cylinder so that the image gets imprinted on the substrate.

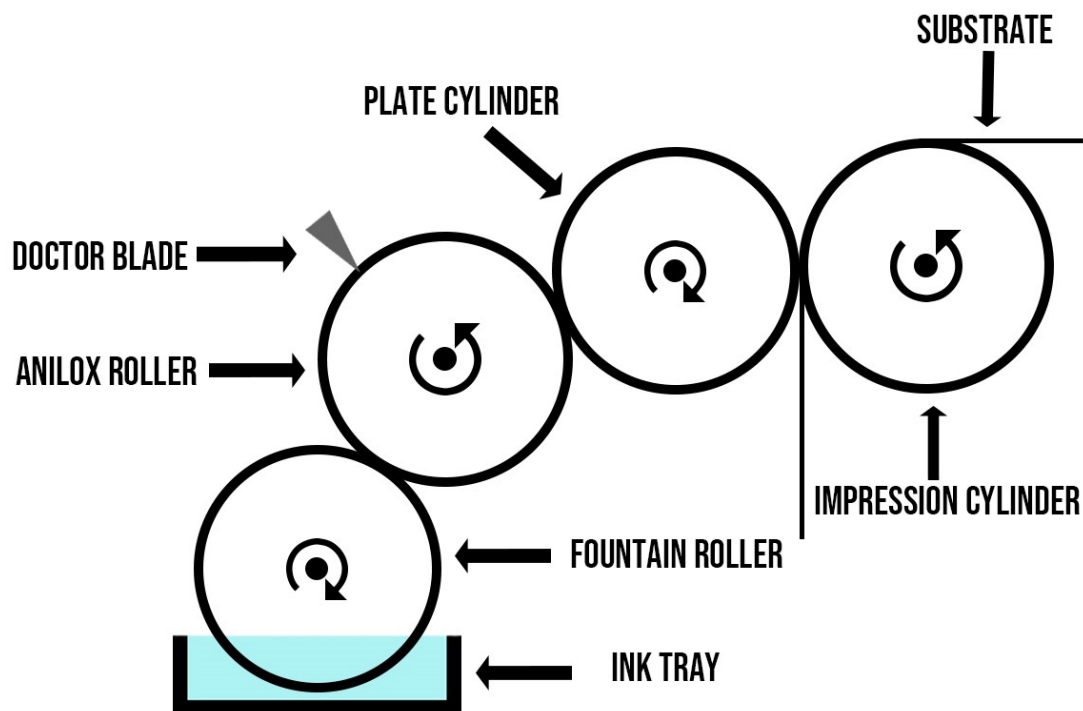


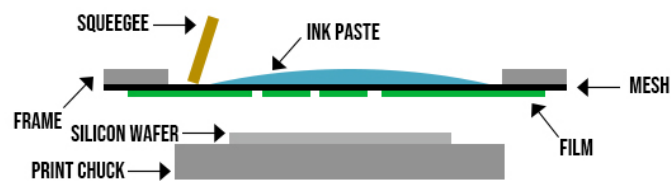
Figure 2: Flexography Printing



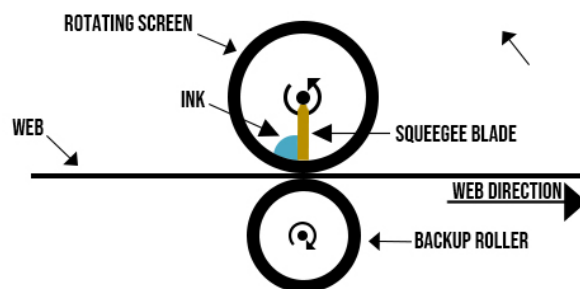
## 2.4 Screen Printing

According to Licari, et al [10] Screen printing is a method of creating sharp-edged images by using stencils (figure 3). The screen is a mesh that could be made of a polymer with a small aperture to achieve the fine degree of detail. Tensiometer is used to check the tension of the mesh and the unit of measurement of the tension is Newton per centimetre N/cm ( $0.101 \text{ kg/cm}^2$ ). Ink permeates through the open area in the screen. A stencil is used to block the negative image. Screen printing is versatile as it can print on different materials such as wood, textiles, electronics. The common types of screen-printing presses are flat-bed, cylinder and rotary. Screen printing is also used for printing conductors and resistors in multi-layer circuits using conductive inks.

The project aim was to develop sensors which can be printed in large volumes roll to roll. Rotary screen printing as explained by Hawkyard, et al [11], can coat higher thickness of an ink, and also helps in the streamlining of the production process as roll to roll printing can be incorporated directly on the main flexographic printing unit and can be used to deposit higher volume of active layer ink or conductive ink if the situation arises.



(a) Manual Screen Printing



(b) Rotary Screen Printing

Figure 3: Screen Printing Technology

## 2.5 Surface Energy and Dyne Level

Packham, et al [12] explain that surface Energy is the excess energy *per unit area* associated with a surface. Surface Energy is fundamental to understand adhesion bonding on a surface. Wetting Tension is a measurable property to evaluate a substrate's surface energy. To acquire the wetting tension of a substrate and determine whether it was suitable to be used for any printing method, dyne level testing method was used.

Dyne level method is a commonly used method to estimate the treatment level of plastic surfaces. It entails the use of solutions prepared from a combination of two chemicals that produce test liquids (dynes) with surface tensions ranging from 30-70 dynes/cm. The test is to drop droplets of several dyne liquids onto the treated surface and watching them spread out over two seconds (figure 4). This method is subjective, but it allows for a quick assessment of the substrate. The polyethylene terephthalate (PET) substrate used in the experiments had a dyne level of 51.4 dynes/cm. The two chemical combinations were Diiodomethane and DI water.

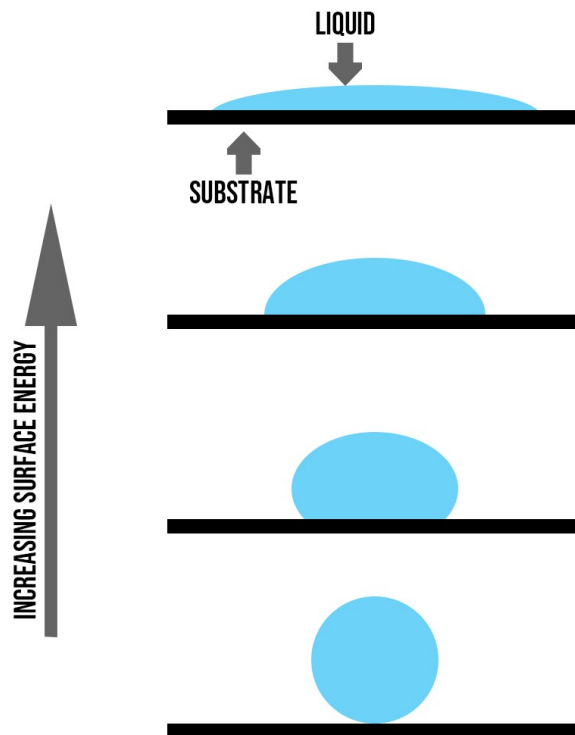


Figure 4: Surface Energy

## 2.6 Conductive Inks and Substrates

The base interdigitated electrode structures can be metals or other substances that make up electrical components. Silver conductive ink was one of the most commonly used inks in multiple different experiments which worked on developing a humidity sensor. Barmpakos, et al [13] discuss the development of a device that can sense temperature and humidity by inkjet printing of Silver Nano Particles conductive ink (Ag solid content: 10–20 wt% , average particle size 20nm) on a paper. Relative humidity of the range 0-90% rH was successfully measured by the sensing module, and linear response was displayed with minimal effect when returning to 0% rH baseline signal (figure 5). A piezoelectric drop-on-demand inkjet printer with a Microdrop MD-K-140 nozzle was used for printing the sensors on a glossy paper.

Interdigitated electrode (IDE) array was the main part of the platform for sensing humidity and temperature. In the range of 20–90% rH with respect to the relative humidity pulses, it exhibited a decent value of sensitivity. [13].

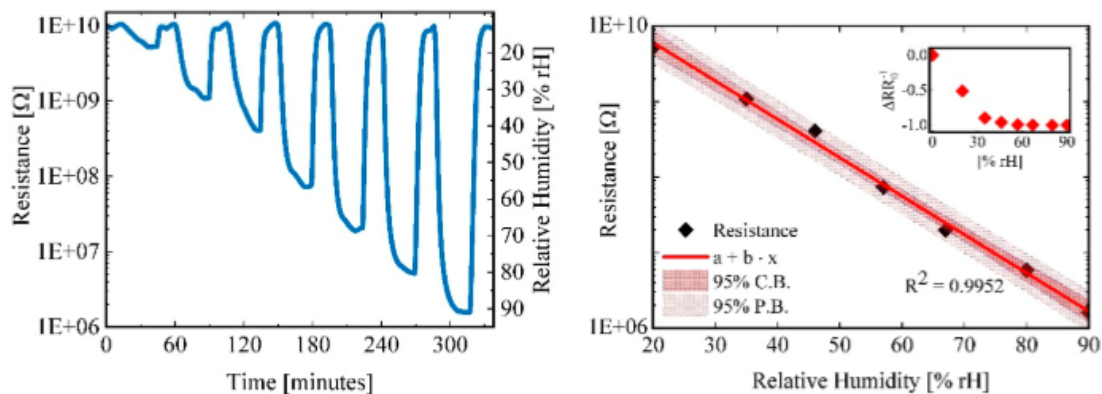


Figure 5: Time and Humidity Resistance Graph [13]

M. Mraović, et al [14], used conductive silver ink from SunTronic to print flat solid plate electrodes on the substrate, which were recycled paper, cardboard and other synthetic materials for comparison such as polycarbonate and Polyethylene Terephthalate (PET) foil. Design structures used were in parallel grid (figure 6).

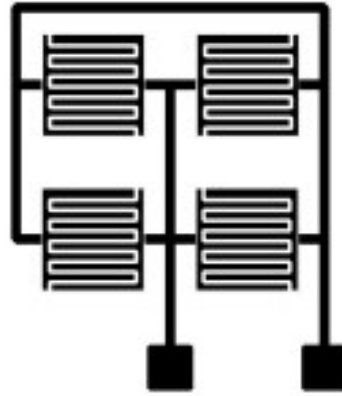


Figure 6: Lateral Sensor Array [14]

These sensors were tested at 23°C and humidity level from 25% to 80% in a humidity chamber. Figure 7 represents the time response of the different material and sizes of the substrates. All the sensors show similar responses and is slightly higher at RH values.

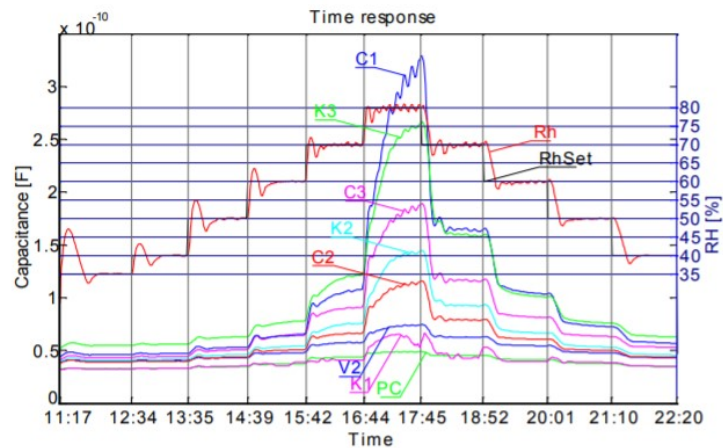


Figure 7: Time Response [14]

Clifford, et al [15] discuss a sensing platform printed using aerosol jet by integrating elements of printed electronics and silicon (Figure 8). Thin humidity sensors films were printed on top of the surface by jet deposition and drop casting. Nano-particle silver ink was used for the interdigitated electrode structure (IDE) deposition which was then diluted with 1:3 parts of deionized water. A convection oven was used to sinter the nano-particle deposition on the printed integrated circuit. This sensor was evaluated in a environmental chamber (Sanyo MTH-2400) at a constant temperature of 20°C.

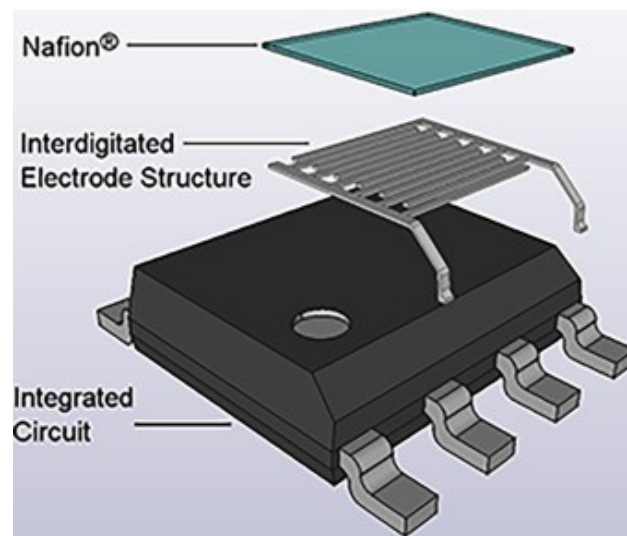


Figure 8: Aerosol jet deposition device structure [15]

Other authors such as Hsiao, et al [16] utilized Silver as conductive ink and Polyimide as the substrate on which  $100\mu m$  gap electrodes were printed via Inkjet printer; and Vasiljevi, et al [17] manufactured sensors using 20 wt% Sun Chemical Ag nano particle ink by ink-jet printing and spin coating.

Gold instead of silver was also used as a conductive ink to develop interdigitated electrodes by Sapsanis, et al [18].  $600nm$  of Au was sputtered on a bare Polyethylene Terephthalate substrate. Mask less etching of the electrode design was performed by laser engraving (Figure 9).

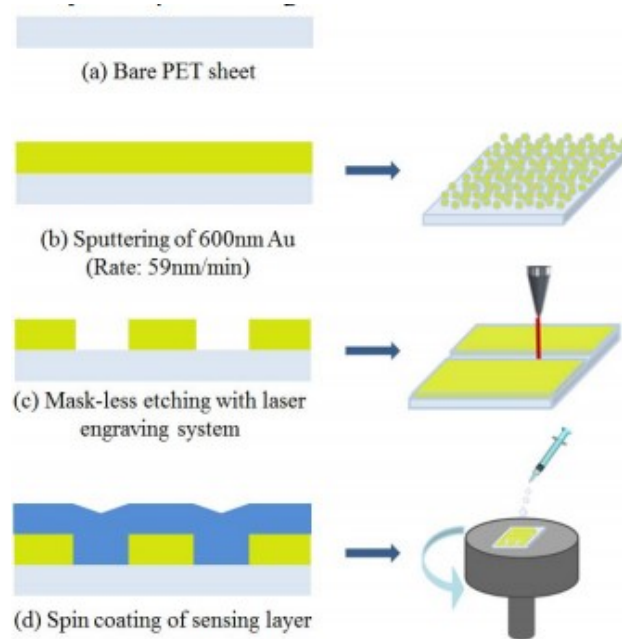


Figure 1: Fabrication steps.

Figure 9: Fabrication process of Au and Nafion based Sensor [18]

## 2.7 Active layer Inks

Multiple research work have been done to develop humidity sensors using Nafion as the active layer on the device [15, 16, 19, 20]. Clifford, et al [15] used Nafion of 20wt% as the active layer in a mixture of water and alcohols of lower aliphatic level. Jet deposition was used to overlay the active sensing material onto the printed layer. Thin Nafion film was coated on top of the integrated circuits which acted as a humidity sensing layer (figure 8). Resistance from pin 2 and pin 4 to the topmost electrode was measured around 16.1 and 18.5 $\Omega$ . The data was collected from the printed sensor from the humidity chamber which was cycled between 80% RH and 40% RH at a constant 20 $^{\circ}$  after a 15 minutes stabilization period. Figure 10 displays the results from the sensor through five cycles.

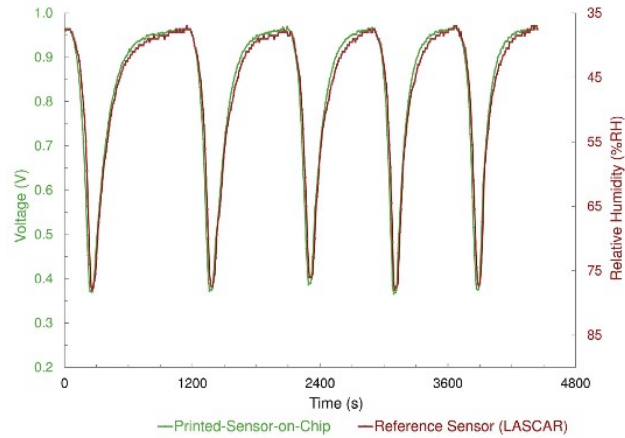


Figure 10: Repetability Characteristics of the sensor [15]

Hsiao, et al [16] also used Nafion, but with a mixture of Titanium Dioxide to improve its reaction time and stability. Apart from using Nafion to sense humidity, nickel oxide was mixed with carbon black to form a thermistor and both materials were fused into a single component to detect both humidity and temperature. A mixture of 0.04g Titanium dioxide and 2g Nafion solution was mixed to form the ink to sense humidity. These sensors displayed stable responses when placed in the humidity chamber and subjected to different ranges of RH (between 40-80% RH) (figure 11). The long term stability was increased by the addition of Titanium di-oxide as it can absorb the intrusion of oxygen into Nafion [16]. At higher RH% it displayed a quick response time of 5s during adsorption.

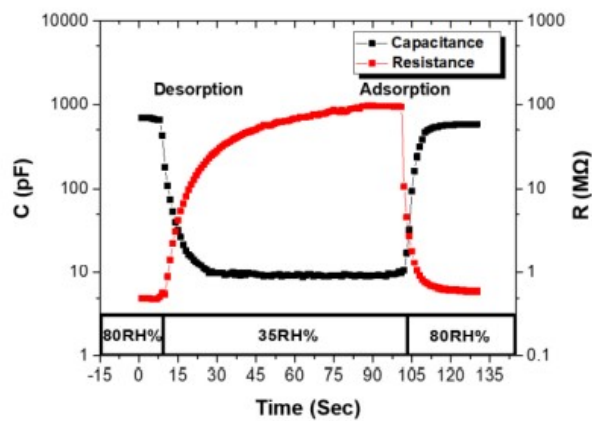


Figure 11: Adsorption and Desorption of Nafion/Titanium oxide sensor [16]

Wang, et al [21] used Nafion in a different approach where it was used as a middle layer with a thickness of 183  $\mu\text{m}$ . The Nafion membrane was cut to size and boiled separately in deionized water and hydrochloric acid, before being soaked in nickel (II)–chelate complex solutions. A spray gun was filled with a diluted silver Nano wire solution and deionized water, allowing for exact control of the flow rate. Silver Nano wires were sprayed across the surface of the Nafion membrane, and the membrane then baked for several minutes in an oven (figure 12). This was repeated 3–5 times until the baked film’s surface resistance was reduced to  $5\Omega$ .

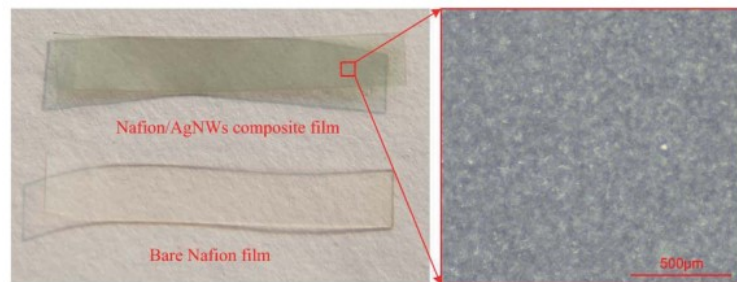


Figure 12: Ag NWs and Nafion Membrane Based Humidity Sensor [21]

When this was tested in a humidity chamber it displayed good electrical response towards organic solvents and surface gases containing water molecules (figure 13). During the change of humidity level from 100% RH to 64% RH it displayed an electrical response of 8mv and had the potential to be used as a breath analyser.

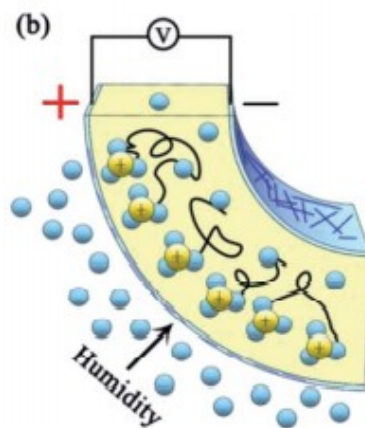


Figure 13: Electrical response mechanism of the Nafion/Ag NWs [21]



Sapsanis, et al [18] used Nafion solution of 5 wt% in a mixture of lower aliphatic alcohol and water. Nafion was then spin-coated on top of Au. Capacitance measurements were taken from the sensor at 1V at four different frequencies. The sensitivity were in the range of frequencies from 1 kHz to 1 MHz. Over 65% RH, at lower frequencies the sensitivity was higher in a linear behaviour (figure 14).

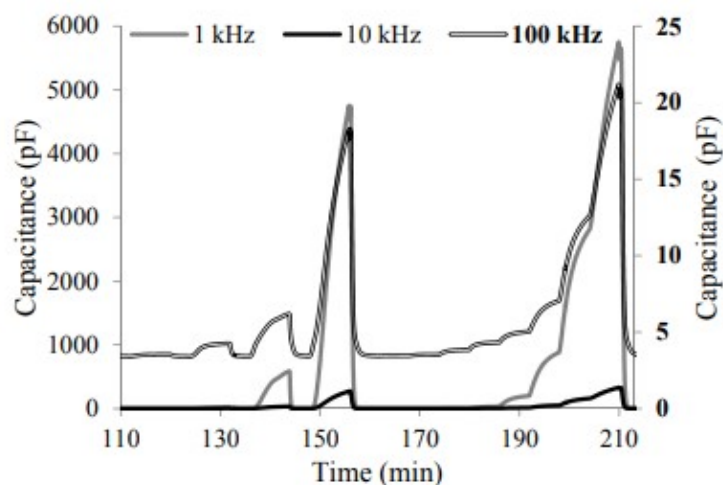


Figure 14: Nafion capacitance versus time at 1, 10 and 100 kHz [18]

**Using Metal Oxides as an active layer:** Among the sensing material used, the other category were of metal oxides which were used for humidity sensing purpose such as  $ZnO_2$ ,  $TiO_2$ ,  $SnO_2$  [22–24]. Ahmad, et al [25] experimented with iron oxides. Using sonicated immersion method, Hematite nanorods structures were produced and deposited on glass substrate coated with fluorine doped tin oxide. This sensor was placed into a humidity chamber to study it's humidity sensitivity.

The sensors displayed an even response to change in humidity from 40% RH to 90% RH without distortion. When tested for repeatability the sensors displayed a extremely stable values (figure 15).

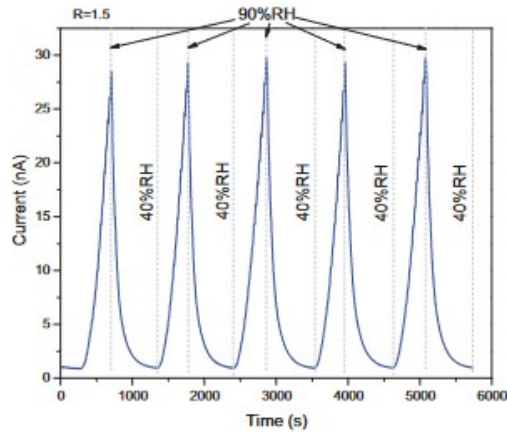


Figure 15: Adsorption and Desorption of Iron oxide based sensor [25]

Graphene oxide has also been considered as an active layer to sense changes in humidity [17, 26]. On top of the electrodes, the second sensor layer was deposited by spin coating three layers of commercially available Graphene Oxide ink with a concentration of 0.4 wt%. These were dried for 30 minutes at 100° and left to cool at room temperature (figure 16).

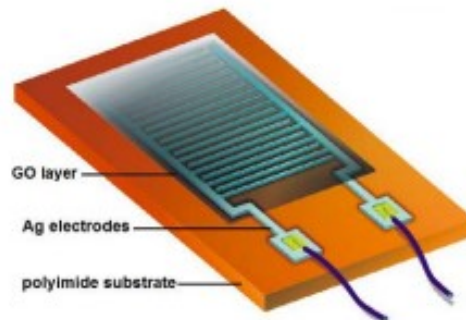


Figure 16: Graphene Oxide based Humidity Sensor [17]

The sensor was placed in a humidity chamber for 9 minutes, resulting in a stable state of 95% RH. The sensors were tested for their capacitance and resistance in the chamber via an LCR meter. The range of resistivity change was observed to be  $2.5M\Omega$  to  $5K\Omega$  from 45% to 85% RH (figure 17). From a study done by Hengchang, et al [27], water molecules are physisorbed by single hydrogen bonding on the hydroxyl groups in G.O sensors as RH rises.

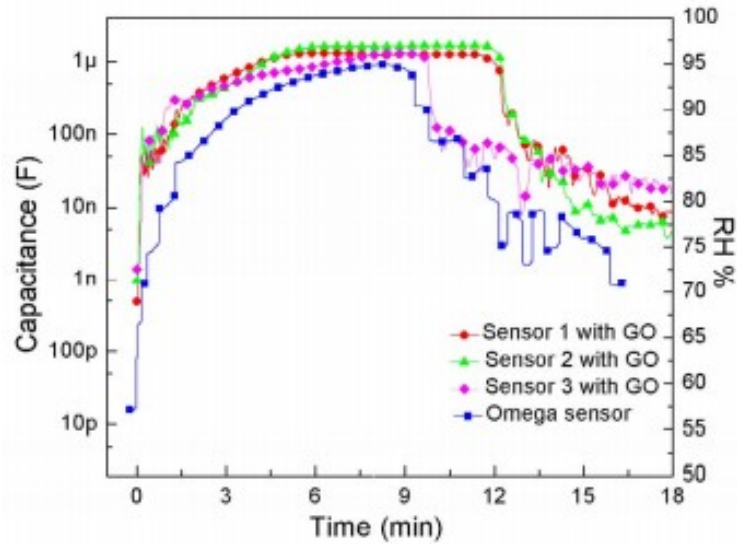


Figure 17: Results of G.O sensor compared to commercial sensor [17]

**Polymer based sensors:** Polymers poly(3,4-ethylenedioxythiophene)-poly(styrene sulfonate) (PEDOT:PSS) was widely used in organic devices according to MacDiarmid, et al [28]. A different combination of inks was demonstrated by Ahmad, et al [29], where they use PEDOT:PSS as conductive ink and polyaniline (PANI) as the active layer [30]. The conductivity could be increased by adding organic solvent such as ethylene glycol. These were printed on a commercial bond paper via an Inkjet printer. During the preparation of these inks, Ethylene Glycol was added.

The printed samples were exposed to three different ranges of 16%, 45% and 90% RH. During testing protonation occurs in nitrogen atoms when water is present. Due to this between de-localization along the polymeric chain, creation of stable polycations takes place which improves electrical conductivity as studied by Nash Cian, et al [31]. Electrochemical impedance spectroscopy (EIS) was used to measure the sensitivity and response time of the said sensor. The humidity was kept constant at both 45%rh and 90%rh. The device displayed a sensitive response of 100% from 45% RH to 90% RH, taking 12 minutes to achieve the saturation state.

## 2.8 Summary

Silver nano particles have been extensively used to print the base electrode structure. Gold has also been used but not to the same extent as silver. Different types of active layers have been tested for their efficiency, when printed on top of the base layer as the sensor layer to react according to its varying properties. The most used material was Nafion in the form of ink. Few research studies used only Nafion as the base ink and few others were done by a varying composition of Nafion with different materials such as metal oxides ( $ZnO_2$ ,  $TiO_2$ ,  $SnO_2$ ) to increase the performance of the sensor. Some designs used only the combination of Polymers such as poly(3,4- ethylenedioxythiophene)-poly(styrene sulfonate) (PEDOT:PSS) by Lovenich, et al [28] and others [29, 30] to develop a humidity sensor.

There were notable common testing parameters done on these sensors, such as the time response of the sensor, repeatability characteristics, and it's change in resistivity according to the conditions which it was subjected to.

Most of the commercially available sensors come with wide range of specification with respect to their mode of operation, such as sensors with broad rH range, operating Supply Voltage ranging from 2V to 24V individually and an output method of either analog or digital, the latter being more commonly used.

The research will focus on the use of flexography method to produce interdigitated electrodes (IDEs) using silver conductive ink and Nafion as the active layer to demonstrate the potential by creating a humidity sensor.

Key points that were reviewed in the literature survey were, conductive inks, different substrates, different active materials, design of Interdigitated Electrode, printing process parameters, testing environments and the response of the device.

The next chapter looks at the experimental methodologies used.

### 3 Methodology

The aim was to develop the Interdigitated Electrodes with the capability of sensing the change in humidity. The experiments focused on how the width and gaps of an Interdigitated Electrode affect the detection of humidity. Surface topographical and electrical analyses were also performed to gain an overall understanding of the performance of the Interdigitated Electrode.

#### 3.1 Equipment used in the study

##### 3.1.1 RK Flexiproofer

The interdigitated electrode (IDE) was printed using an RK Flexiproofer 100 (Figure 18) which is a benchtop flexographic printer, with a print speed of 20 – 99m/min. The engagement can also be adjusted between the substrate and plate. It has a maximum printing area of 240x75mm.

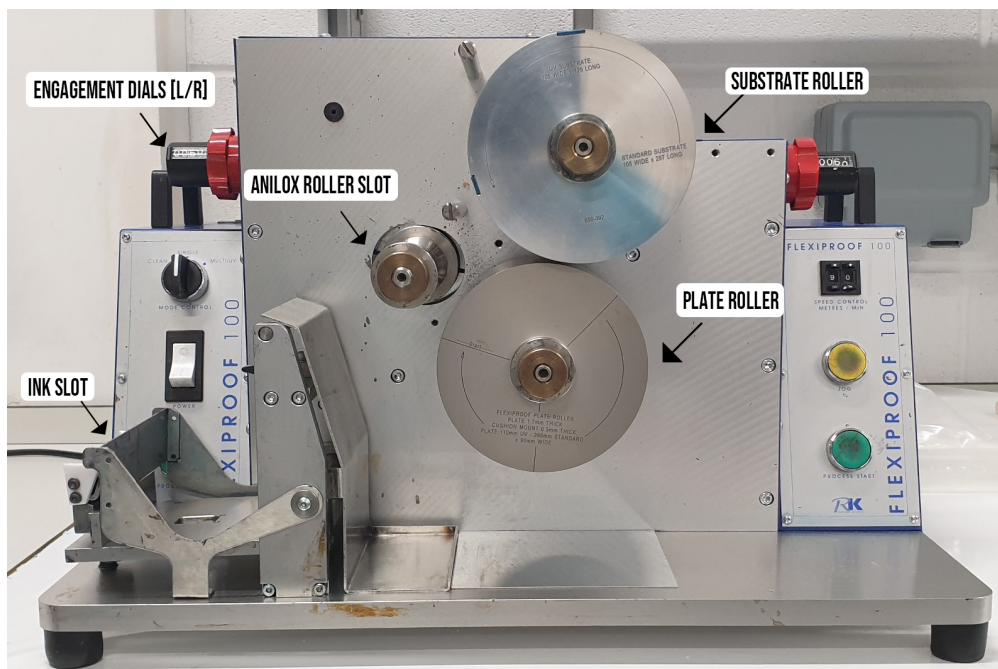


Figure 18: Flexiproofer

### 3.1.2 Anilox Roll

Anilox roll (figure 19) meters the transfer of ink from chamber to plate. The pattern and the cell volume of an anilox roll determine the quantity of ink transferred.

The most common engraving in the anilox rollers is the  $60^\circ$  hexagonal pattern which has advantages over  $45^\circ$  and  $30^\circ$  engravings (figure 20). It has proved best to split a surface into spaces of equal area using honeycomb structure or a hexagonal grid. The  $60^\circ$  pattern allows the cells to efficiently distribute the volume compared to  $45^\circ$  engraving.

The anilox used were of cell volume of  $8\text{cm}^3/\text{m}^2$  and  $14\text{cm}^3/\text{m}^2$ . The anilox with the cell volume of  $8\text{cm}^3/\text{m}^2$  has 100 cells per linear cm and the  $14\text{cm}^3/\text{m}^2$  cell volume anilox has 75 cells per linear cm.



Figure 19:  $8\text{cm}^3/\text{m}^2$  Anilox

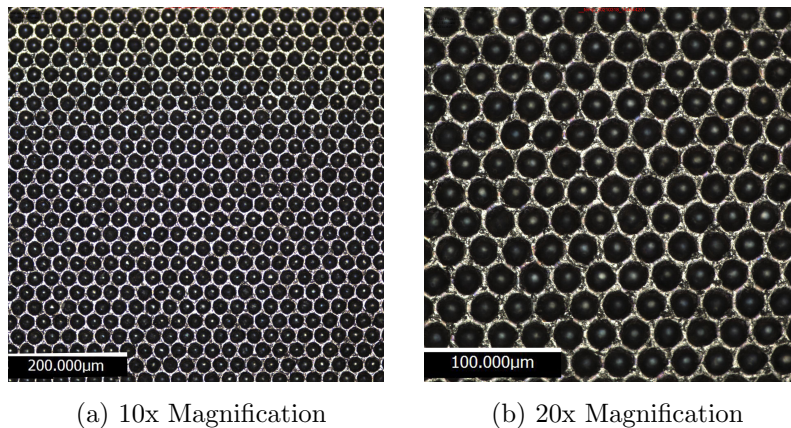


Figure 20:  $8\text{cm}^3/\text{m}^2$  Anilox Closeup

### 3.1.3 3D Microscopy Alicona

The microscope images of silver electrode were obtained on the Alicona Infinite Focus G5 microscope (Figure 21). It is a flexible optical 3D measurement system. It was used to verify dimensional accuracy and measure the surface roughness of the printed features. A white light source is inserted into the optical path of the system and beamed onto the sample. Depending on the surface of the sample, the light is reflected into different directions and is focused onto a light sensitive sensor behind a beam splitting mirror, as shown in figure 22 [49]. By analysing the variation of focus along the vertical axis the algorithm converts the gathered sensor data into 3D information. This instrument allows the user to gather surface data from a horizontal plane to vertical up to 90°.

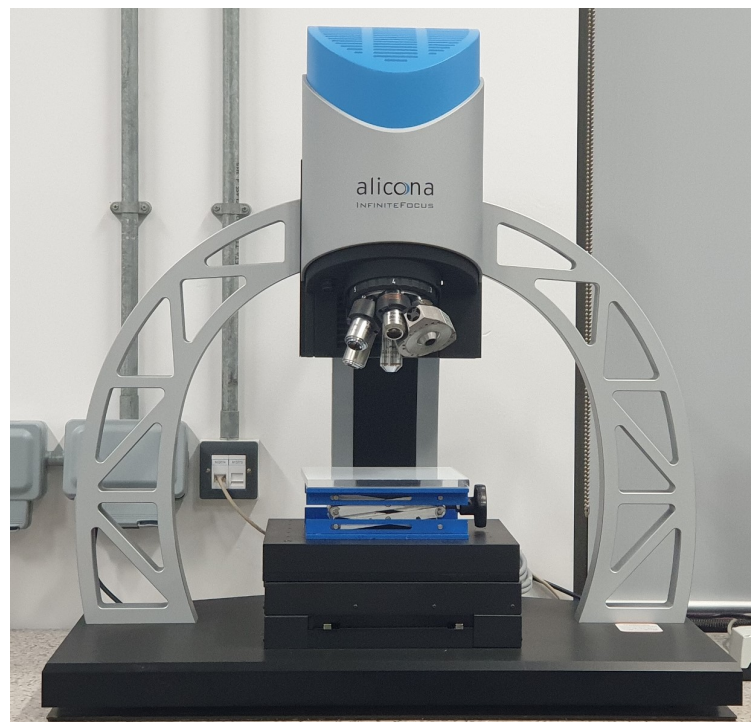


Figure 21: Alicona 3D Microscope

Real3D is a full form measurement algorithm, which merges the single measurements into a full 3D dataset. The sample is measured at various tilt and rotation angles, these are then transformed into a co-ordinate measurement system. These single measurements are merged into a final 3D data set.

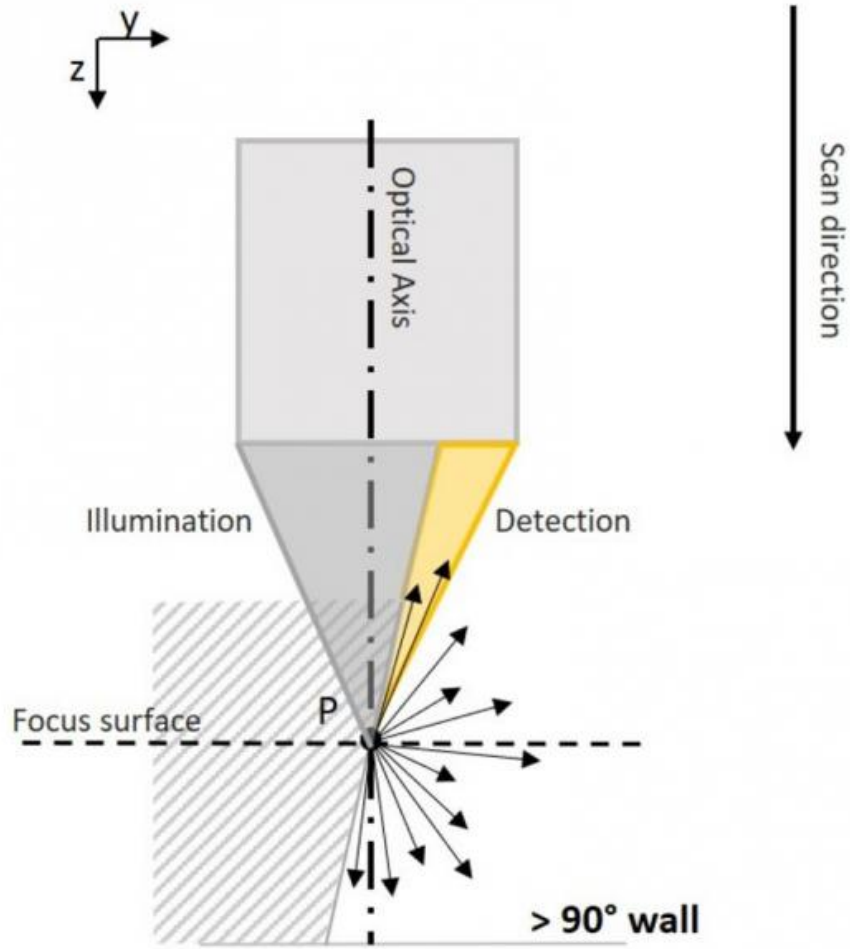


Figure 22: Optical 3D measurement schematics [49]



### 3.1.4 Wyko Veeco Surface Profiler

The other method used to analyse the printed substrate was non-contact Whitelight Interferometry (WLI), Wyant and James [32]. There are 3 methods for the WLI namely 1: diffraction grating interferometers, 2: vertical scanning or coherence probe interferometers, and 3: white light scatter plate interferometers. In this research, the vertical scanning method was used.

In the vertical scanning method, the white light beam from the source initially passes through a filter of neutral density that maintains the white light's short coherence. A beam splitter then splits the beam into two parts; one part is guided by an objective lens and interferometer toward the sample, and the other part toward a reference mirror. Only a shallow depth of field is in focus due to the short coherence of the filtered light source. The sensor head scans over a vertical range. This produces a series of patterns of interference which are collected to create interferograms by a charge-coupled device (CCD) camera (figure 23). To assess the surface height of each pixel by calculating fringe coherence, the interferograms are then analysed by a computer program. Multiple data points from the same area can be extracted from the specific region of the printed substrate for analysis.

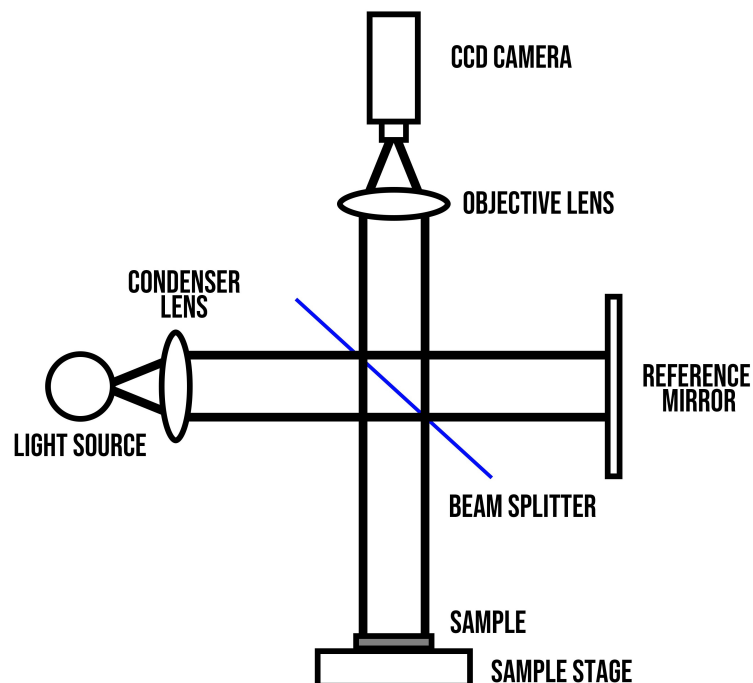


Figure 23: Whitelight interferometry schematics

Wyko Veeco NT9300 series uses non-contact White Light Interferometry method to profile the surface (figure 24). It has a vertical measurement range of 0.1nm to 10mm, lateral spatial sampling of 0.1 to  $13.2\mu\text{m}$ , and has magnifications of 1.5X, 2.5X, 5X, 10X, 20X, 50X. Using its software called Wyko Vision, analysis of the substrate can be done which uses phase shifting algorithm to acquire the data.

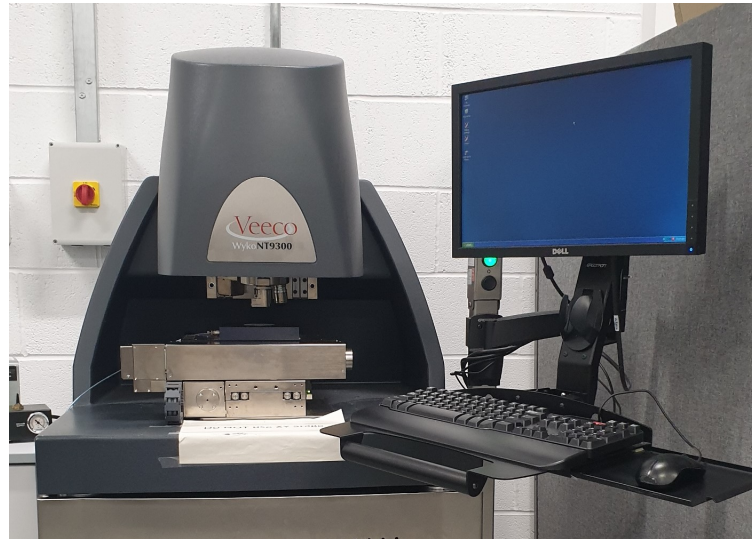


Figure 24: Wyko Veeco NT Series

### 3.1.5 Kinexus Pro Plus Rheometer

The study of deformation and flow of matter (of both solids and liquids) is known as Rheology. This machine can be used in the modes of stress control, shear rate control and direct strain-controlled oscillation. It uses rSpace software which can be customized to the required type of sequence driven strain test. Gels, emulsions, pastes, dispersions can be measured on this rheometer.

Barnes, et al [33] state that 'When parts of liquid show no signs of slipperiness it creates resistance which is proportional to the speed at which the parts of the liquid are separated from each other'. Viscosity is this lack of slipperiness. It can also be measured as resistance to flow. Fluids fall under two categories namely Newtonian and non-Newtonian. Newtonian liquids do not change their viscosity under pressure, whereas non-Newtonian fluids do. An example being water for Newtonian and Ketchup for non-Newtonian fluids. Viscosity of an ink can be used to co-relate it's behaviour while printing. Depending on the type of printing method used, the viscosity of an ink should be preferably controlled for its environment. As an example, gravure printing inks are characterized by higher viscosity, Izdebska-Podsiady, et al [8].

Cyan ink was initially used on the Rheometer instead of Silver, as silver was a self-sintering ink and would damage the equipment. Test performed on the cyan ink was parallel stress based. Parallel plates were used to measure the rotational constant sheer, where the gap can be adjusted. Roughened plate of 40 diameter was used. Two tests were performed, which was a gap test and a shear rate test. Gap test was performed to select the optimal gap to minimize wall slip. In figure 25, 4 gaps were selected to check which one of them was the most optimal. Shear rate test was performed next to understand the behaviour of cyan ink in its change of viscosity over a period with applied parallel stress.

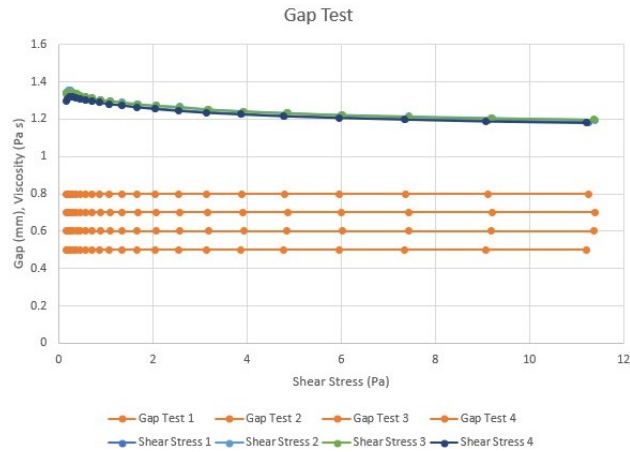


Figure 25: Gap Test

In figure 25 X-axis represents the shear stress, Y-axis represents gap in mm and viscosity in  $Pa.s$ . In figure 25 the four orange lines indicate the four different gaps 0.8, 0.7, 0.6 and 0.5mm between the parallel plates. The comparative results shows that the difference in the shear stress is negligible between the different gaps. 0.6 millimetre was selected for the shear rate test.

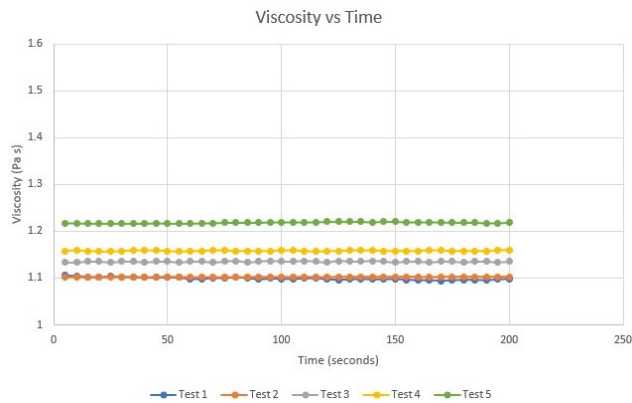


Figure 26: Viscosity vs Time

In figure 26 the X-axis represents the time in seconds, Y-axis on the left represents viscosity in  $Pa.s$ . Shear rate is the controlled variable. All the four lines represent the same ink but set to different shear rates. From the first two tests, the ink has the same viscosity behaviour at  $1.1 Pa.s$  but it slightly increases from 1.1 to  $1.134 Pa.s$  in the third test. As the progression of the tests take place for the four different shear rates, the slight increase in viscosity of the cyan ink is negligible and the ink is not susceptible to shear thinning or

shear thickening during a prolonged usage period while printing.

## 3.2 Materials

The focus was to develop the Interdigitated Electrode design capable of sensing the change in humidity. How the width and gaps between the fingers of the Interdigitated Electrodes affected the detection in changes of its humidity was also investigated.

The materials and apparatus used are discussed such as inks, substrates. Surface topographical and electrical analyses is also performed which shows overall understanding of the performance of the type of Interdigitated Electrode that was being developed.

### 3.2.1 Substrates

Plastic films considered for printing were Polypropylene(PP) and Polyethylene terephthalate (PET) [34]. Polypropylene (PP) as explained by Karian, et al [35] is a plastic of high gloss, clarity and high tensile strength. Commonly used type of PP is cast un-oriented polypropylene (CPP) since it has higher impact and tear resistance. Compared to Biaxially oriented polypropylene (BOPP) it has lower stiffness, higher elongation and higher haze.

For the experiments Polyethylene Terephthalate (PET) was selected (Table 1) since it can maintain it's physical properties over different temperature ranges [36], has low moisture absorption and has better electrical conductivity properties compared to PP.

Table 1: Substrate

Name	Description
Melinex 339	0.175mm Matt White Polyethylene, Manufactured by DuPont Tejin Films
Dyne leve	51.4 dynes/cm

### 3.2.2 Cyan Ink

UV flexo inks have good physical and chemical resistant properties. They also have fast curing process and can achieve better output of quality when compared to water and solvent-based inks, Rebros, et al [37]. Since these inks only cure when exposed to UV light at high intensity, cleaning is easier.

Solarflex Nova SL process cyan Ink from Sun chemical was used to establish the required engagement on the RK Flexiproofer before using the Silver Ink to avoid wastage. Rheological properties were studied to make sure that the ink was not susceptible to changes in properties during a prolonged period of printing on RK Flexiproofer. The ink was cured on a UV conveyor belt dryer.

### 3.2.3 Conductive Inks

Conductive inks are made up of nanoparticles linked with each other with solvents. These solvents evaporate during drying. These inks are high in conductivity, such as Gold, Silver or Copper. Silver ink PFI-500 from NovaCentrix was used (Table 2) which is water based nano silver ink for flexography. This water-based ink was dried in a convection oven for 8 mins to cure at 120° Celsius.

Table 2: PFI-500

Name	Description
Silver Content Wt%	50 (+/- 2)
Density (Wet)	1.88 g / ml
Viscosity @ 10s <sup>2</sup>	400-800 cP
pH	5.88 to 5.94
Volume Resistivity	7 - 9 $\mu\Omega$ cm
Printed Sheet Resistance	100 - 600 m $\Omega$ /sq (Anilox and Cure condition dependant)
Coverage	120 - 700 m <sup>2</sup> /kg (Anilox Dependant)

### 3.2.4 Active Material

**Polymers:** Polymer described by Young, et al [38] is a substance which has large molecular structure made of multiple chemical units called monomers which are held together to make long chains. Polymers are found everywhere in the daily objects such as in clothes, food and other goods. Changing the macroscopic properties and chemical structure allows the user to design the polymer material. Polymerization is the method through which polymers are created.

Synthetic polymers are made from artificial components through a series of chemical reactions. Silicone, nylon, polyethylene are some examples of synthetic polymers. There are polymers which have conducting properties which are known as intrinsically conducting polymers (ICP) which have high electronic conductivity and high electron affinity. ICPs have been long used in applications such as in the development of biosensors [39]. ICP provide an excellent signal communication in molecular detection due to their electrochemical activity towards molecular interaction and high sensitivity in conductivity. Incorporation of secondary material such as nano particles, ions or nano wires of metal oxides, carbons, metals into polymers [16,24] are some good examples of ICPs.

**Nafion:** Nafion studied by Mauritz, et al [40] is a sulfonated tetrafluoroethylene-based copolymer which has conductive properties. Nafion can be used as an electrode modifier for sensor fabrication. Nafion helps to block the anionic species from reaching the electrode surface and allows the cation conduction to pass through, thus leading to good selectivity. Nafion's hydrophilic negatively charged sulfonate group enables good conductivity in the presence of humidity.

Nafion perfluorinated resin solution in the form of ink from Sigma Aldrich (Table 3) was selected as the active layer to be printed on top of the Silver IDEs using Flexiproofer with  $24\text{cm}^3/\text{m}^2$  anilox and dried at room temperature for few hours, to achieve the conductivity response with respect to the change in humidity. Figure 27 represents structure of Nafion.

Table 3: Nafion Specification

Nafion Version	Sigma Aldrich 663492
Appearance (Colour)	Colourless
Appearance (Form)	Liquid
Solid Content	20-22 % wt
Water Content	32-36 % wt
1-Propanol	42-46 % wt
Ethanol	2 % wt

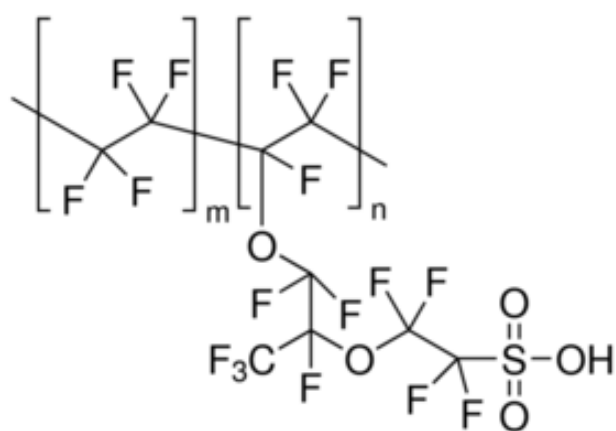


Figure 27: Nafion Perfluorinated Resin Structure



### 3.2.5 Printing Plates

Photopolymer plates [41] are used to print on Flexographic machines. These plates are used to transfer the ink and image to a substrate. The quality of the image is dependent on the quality of the plates. Polymer plates of  $175\mu m$  Macdermid ITP60 Lux of 3.2k dots per inch (dpi), white area of 73% and ink coverage of 27% with a Plate relief height is 1.2mm were used (Table 4). The plate dimensions are 260mm along and 85mm across.

Table 4: Printing Plate

Name	Description
Plate Name	MacDermid ITP60 Lux
Thickness	$175\mu m$
Resolution	3.2k dots per inch
White Area	73%
Ink Coverage	27%
Plate Relief Height	1.2 mm

The plates were analysed by White Light Interferometer (WLI) machine to check their width and accuracy. Average width of 6 fingers at different locations from every Interdigitated Electrode (IDE) on the three different plates was measured. Plates 200, 300,  $400\mu m$  track width consisting of 20 IDEs each were profiled, for an average of all 20 IDEs from each single plate (table 5).

Table 5: IDE Width on Plate Design vs Actual

Designed IDE Track Width	Actual IDE Track Width
$200\mu m$	$204.08\mu m$
$300\mu m$	$306.80\mu m$
$400\mu m$	$404.42\mu m$

### 3.2.6 Interdigitated Electrode Structure and Plate Design

Since its introduction in the 1970's the Interdigitated Electrode structure has been widely used in many areas, Vakilian, et al [42]. It was able to meet the growing demand of Lab-on-Chip (LoC) devices low production cost. The efficiency of the structure depends on the gap between the two structures and the general design depending on its use.

A multiple interleaved finger type structure was used for these experiments (Figure 28), with the width of 16.5mm and length 22mm. This type of interdigitated electrode structure provides two electrodes with a small gap which allows it to be operated using smaller voltage compared to regular electrodes. It also increases the sensitivity of the device to external parameters that affect the capacitance.

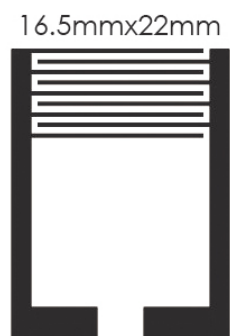


Figure 28: IDE structure [Track Width:300 $\mu m$ ][Gap:500 $\mu m$ ]

Plates were designed with IDEs Track width of 400,300 or 200 $\mu m$ . Each of the plates had 4 sets of IDEs with the gaps of 100,200,300,400 and 500 $\mu m$ . The interdigitated electrodes dimensions are of 16.3mm along and 22mm across. Purpose of having multiple IDEs is to test and determine which gap and width configuration of the Interdigitated Electrodes have the best performance during testing.

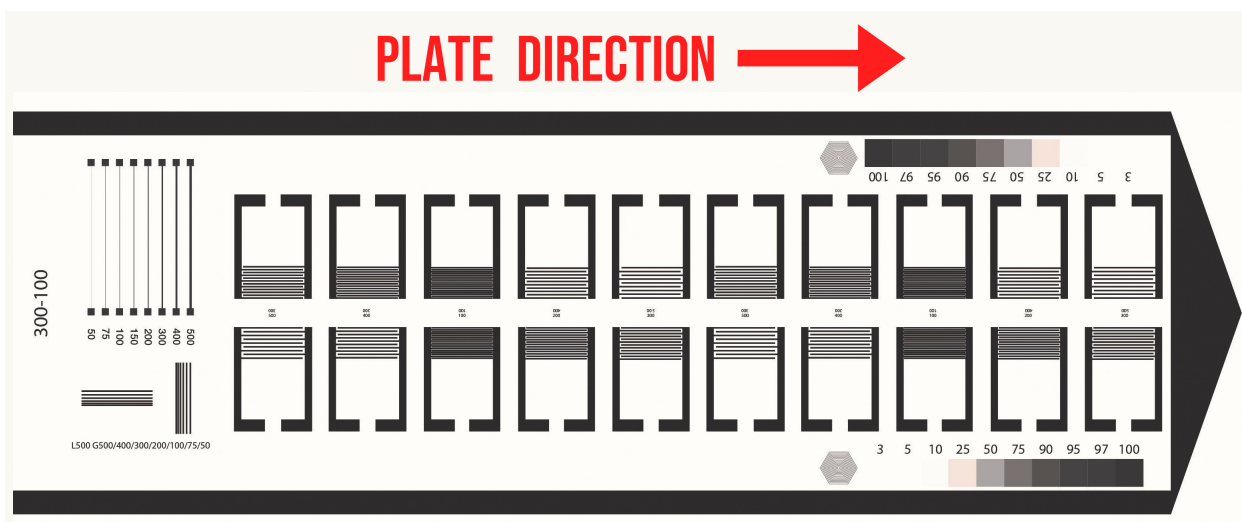


Figure 29: Base Layer Plate Design [Track Width:300 $\mu m$ ]

Base Layer plate (Figure 29) is used to print the IDEs using silver ink. Top layer plate (Figure 30) is used to print Nafion on top of the IDEs which will act as an electrode modifier which is hydrophobic and allows the circuit to detect change in humidity during the experiments.



Figure 30: Top Layer Plate Design

## 4 Printing Interdigitated Electrodes

### 4.1 Introduction

Sensor fabrication and design was influenced from [17]. The sensor construction (Figure 31) consists of Polyethylene Terephthalate (PET) as the substrate, conductive silver ink as the structure of the electrode printed onto the substrate and Nafion in the form of ink printed on top of the electrode to sense the change in Humidity. Initial prints were taken on the RK Flexiproofer using process cyan ink to establish the required engagement between the substrate and plate to avoid wastage of silver ink.

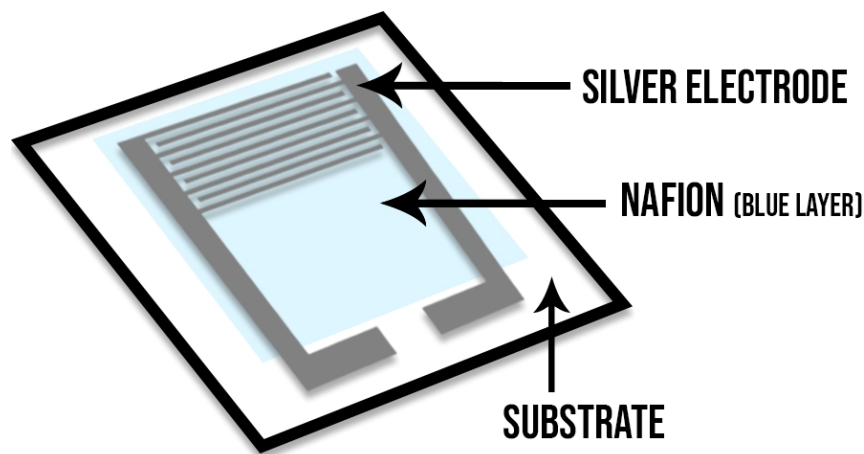
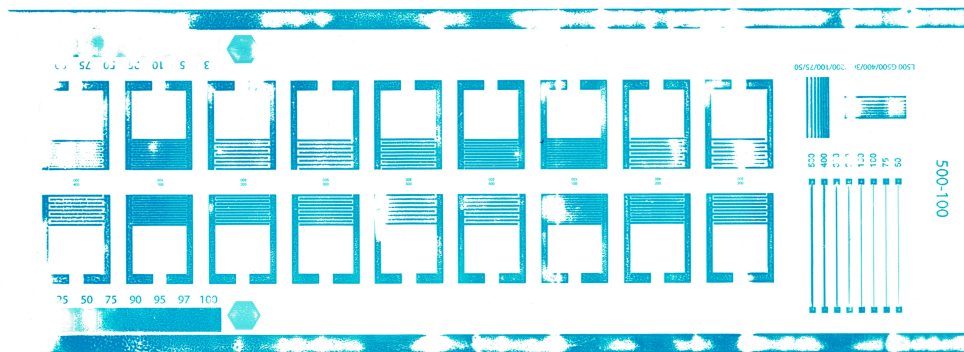


Figure 31: Sensor Structure

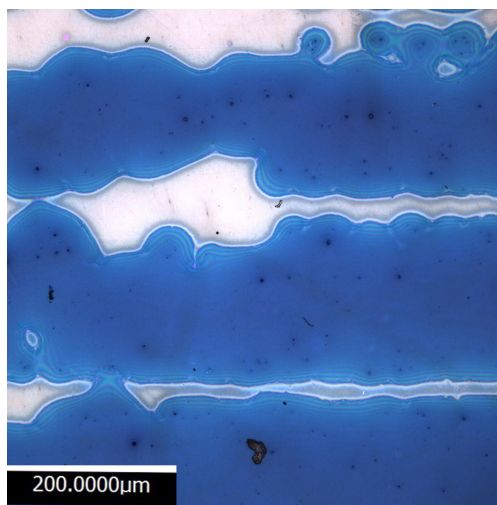
Once when the engagement on the RK Flexiproofer had been determined by checking if the cyan electrode prints were according to the plate design (gap and width of the cyan print inspected on the Wyko surface profiler), the second stage of the sensor fabrication was to use the silver and print the electrodes. They were tested for their electrical resistance via a digital multimeter, for all the gaps and widths. Third stage was to print the Nafion on top of the silver electrode, left to dry and placed into the humidity chamber at a range of 40% to 80% relative humidity to observe the changes in the resistance according to the change in humidity.

## 4.2 Optimization of print settings using process cyan ink

Initial prints were taken on the RK Flexiproofer using process cyan ink to establish the required engagement between the substrate and plate. The initial engagement (image transfer) began at 120 clicks on the engagement dials for both Anilox and Substrate engagement, this was considered as the kiss-touch engagement (K). At the K position, the prints displayed a very poor engagement (Figure 32 a, b) between the rollers leading to the prints having either no contact in certain places or prints with pin holes.



(a)

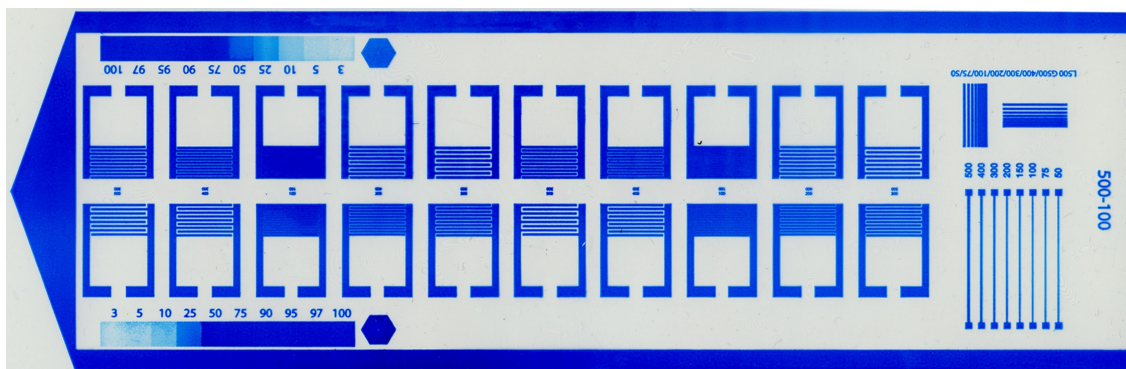


(b)

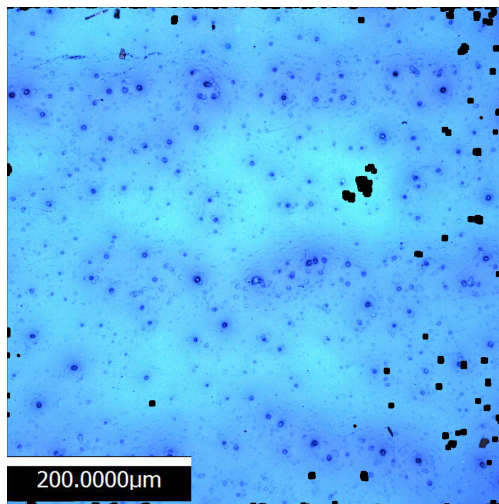
Figure 32: Cyan print with patches when using insufficient engagement

White patches are present on both Interdigitated electrodes (Figure 32(b)) and on the outer chevron bands which indicate insufficient engagement (Figure 32 (a)).

Pressure setting ranging from 80 clicks and below on the engagement dials had high engagement between the instrument and displayed the prints with either fingers overlapping on the IDE or ink bleeding on the edges. Due to excess pressure, the prints display darker shade of cyan ink (Figure 33 (a)) along with most of the IDEs having their fingers merged (Figure 33 (b)).



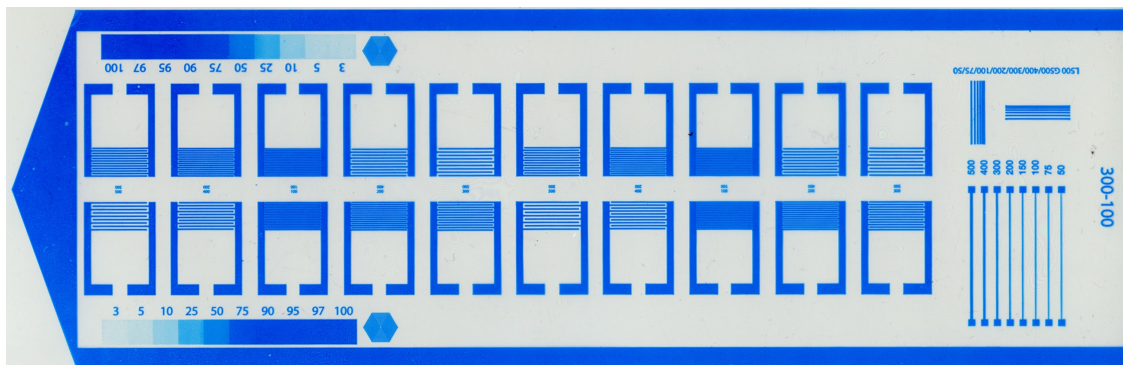
(a)



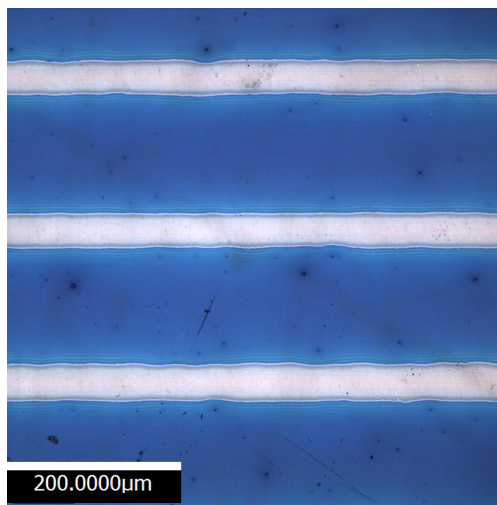
(b)

Figure 33: Cyan Print with excess Ink

From analysing multiple prints taken using the pressure setting at K-20 clicks, it was observed that the prints obtained were of required quality.  $40m/min$  speed on the Flexiproofer was found to be optimum as it did not result in ink splashing or over deposition of ink. These prints did not have any bleeding or pinholes similar to the ones seen in figure 32,33. The figure 34 (a,b) displays the quality of prints obtained at these pressure setting and speed. This required engagement was noted as K1. The UV Cyan ink prints were cured using SC Technical Services conveyor dryer.



(a)

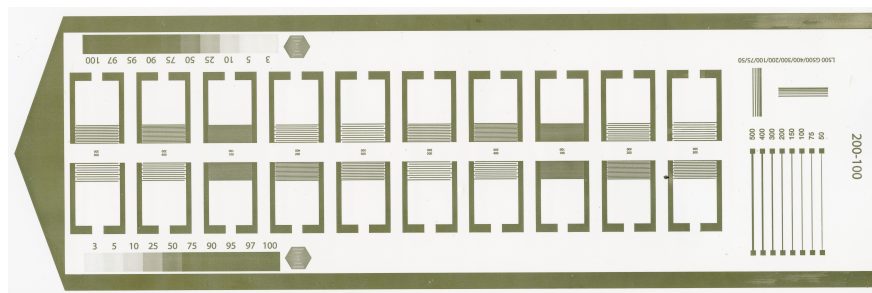


(b)

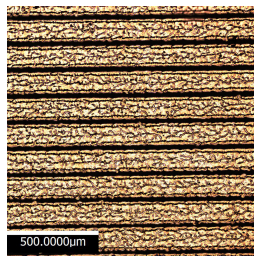
Figure 34: Good cyan print

### 4.3 Print Quality of Silver

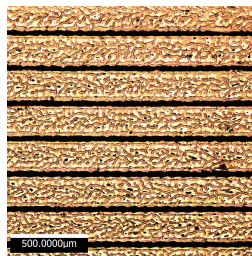
Based on the analysis of the cyan prints taken using the pressure setting at K1 (Table 6), the same K1 pressure setting was used to print silver. Silver printed substrates were cured in a conventional oven at 120° for 7 minutes. These prints did not have any bleeding or pinholes but resulted in producing a good quality set of prints. Figure 35 is an example representation of the required silver IDE print quality. The branch like structure on the fingers (Figure 35(b, c, d)) is a common occurrence in printing where the rolling motion of the anilox lifts up the ink deposited at the end of the motion (Figure 35d).



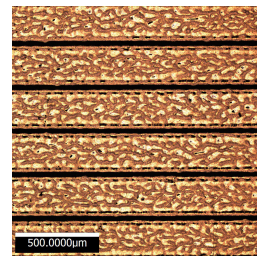
(a) Silver Print (Track Width:200 $\mu$ m)



(b)



(c)



(d)

Width:200 $\mu$ m,Gap:100 $\mu$ m Width:300 $\mu$ m,Gap:100 $\mu$ m Width:400 $\mu$ m,Gap:100 $\mu$ m

Figure 35: Good silver IDEs examples

Table 6: Flexiproofer Settings

Anilox Engagement Dial Value	100
Plate Engagement Dial Value	100
Speed	40m/min



## 4.4 Profiling of Printed Silver IDE

The prints were analysed for their width, gap and height to check the accuracy of the printed IDE dimensions and to check if the fingers are overlapping or making contact in any regions. For an Interdigitated Electrode (IDE) using the interleaved finger design, the closer the fingers are, the better it works in detecting change in parameters. Using flexography to print these small IDEs creates a challenge where it can only be printed until a limit after which if it's gets smaller, the fingers overlap and makes the IDE unusable. This is one of the limitations of using flexography to print small sensors.

Profiling these IDEs gave an estimation as to the smallest size limit that can be reached without the fingers making contact. Interdigitated Electrodes of the 3 different sizes were printed using silver over white Polyethylene terephthalate (PET) substrates. These Interdigitated Electrodes were then analysed for their width and gap of the fingers, using White Light Interferometer (WLI). One of the disadvantages of using the silver ink was that while printing, it tended to dry in the anilox which allowed only few prints per print run due to the machine stopping after every print run for few seconds, unlike a traditional printing machine where the prints are continuous.

After printing, the sample was selected and placed under the White Light Interferometer (WLI). Interdigitated Electrodes (IDEs) with same gap were selected from start, center and end sides of a print, as the dimensions of IDEs might vary from one end to another, due to speed at which the silver ink dried.

In a print, selected from the 3 different IDEs, 5 random points from each IDE were selected since every single point on the IDE might not have the same profile. These 5 points were profiled for their width, gap and height and an average was taken for each IDE. These 3 different IDEs were then compared to each other and checked for variations. Figures 36 is an example representation of how the IDEs were selected for their track width and gap profiling, where the red dots represent the example measurement locations.

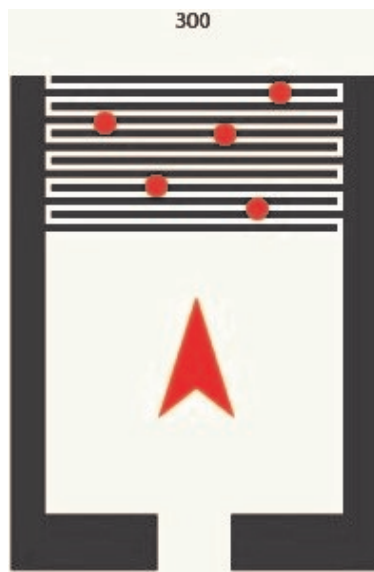


Figure 36: Example representation of selecting random regions

## 4.5 Silver Print Setup Analysis

Three different plates were used to print the silver Interdigitated Electrodes (IDEs), each plate being a different width for the interdigitated electrode (IDE) which are  $400\mu m$ ,  $300\mu m$  and  $200\mu m$ . Each plate had 4 identical sets with gaps between the fingers ranging from  $500\mu m$  to  $100\mu m$  (figure 37).

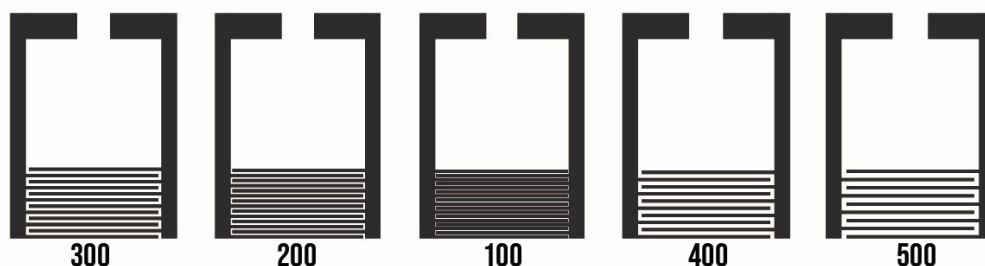


Figure 37: Example of an IDE set

While printing the silver ink, from the two anilox used,  $8cm^3/m^2$  volume anilox performed the best, as the printed Interdigitated Electrodes (IDEs) dimensions were most accurate. The  $14cm^3/m^2$  volume anilox deposited more ink which led to inaccurate dimensions of the IDEs. Fingers of IDEs with the  $200\mu m$  and  $100\mu m$  gap also merged which made them unusable. Hence  $8cm^3/m^2$  volume anilox was used.

Upon inspection under the microscope, multiple IDEs of the gaps  $100\mu m$  from different prints have fingers merge at random locations which made them unusable (figure 38). IDEs with the dimensions above  $100\mu m$  gap were selected for further testing.

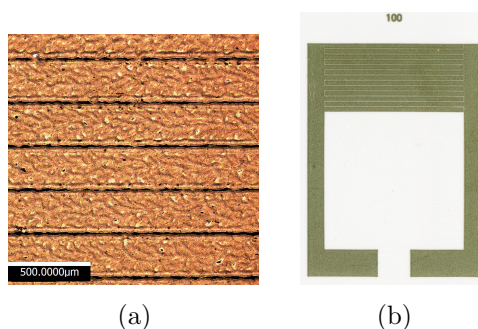
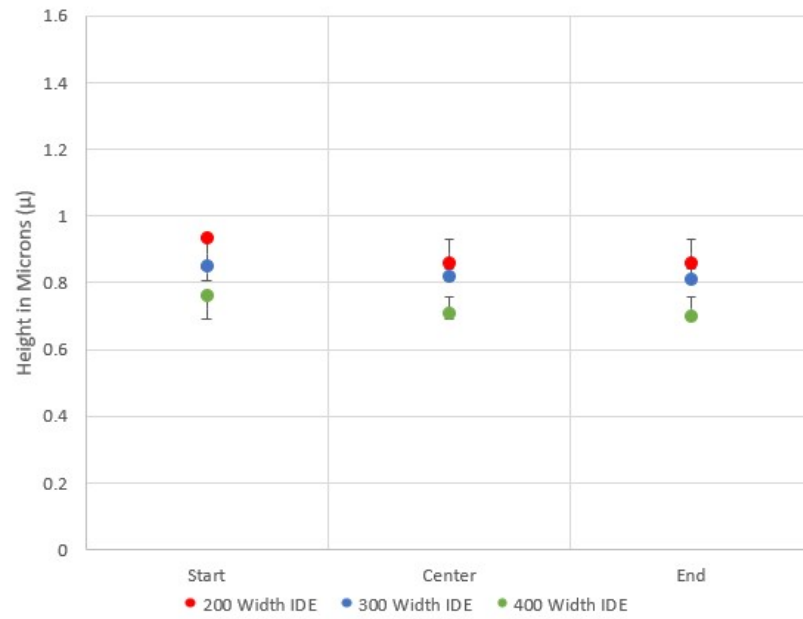
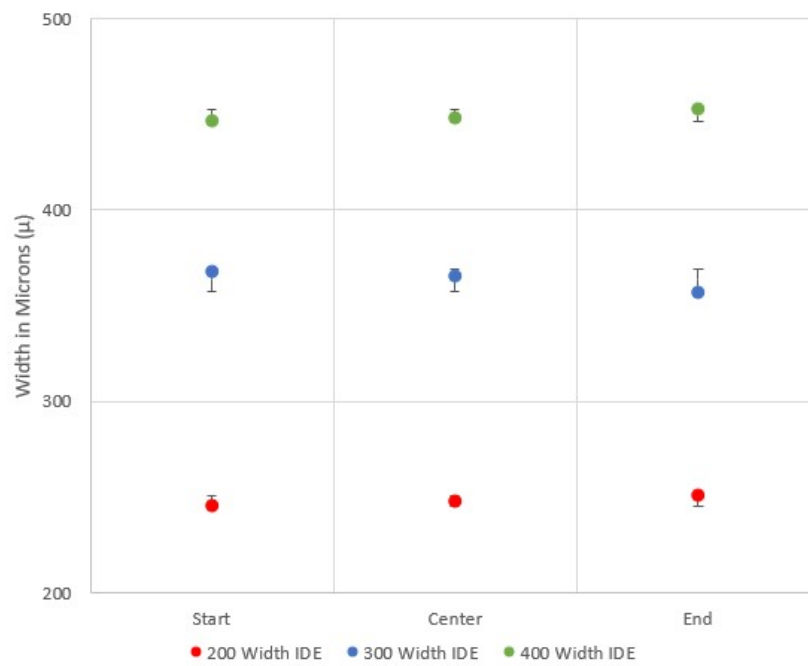


Figure 38: IDEs Fingers Merging [Track Width: $400\mu m$ , Gap: $100\mu m$ ]



(a) Height



(b) Width

Figure 39: Scatter Plot Representing printed silver height and widths of different IDEs

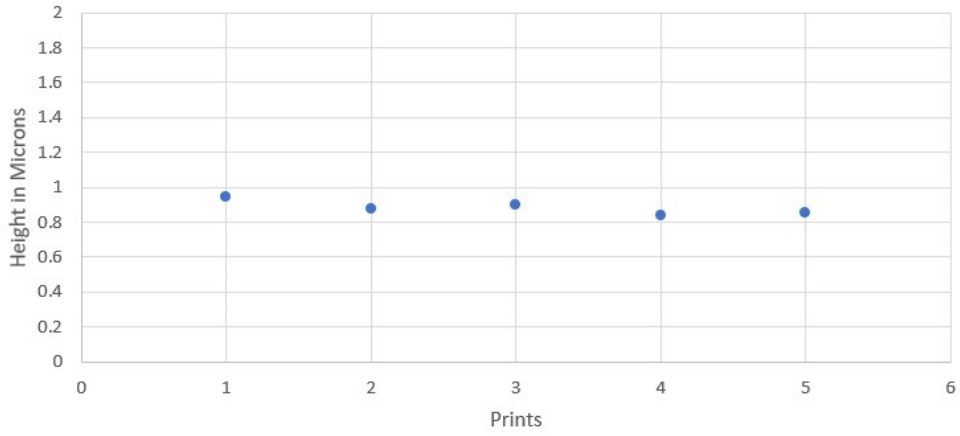
In figure 39, X axis represent start, centre and end Silver Interdigitated Electrodes (IDEs) on a print, Y axis represent the Height and Width of the IDE in  $\mu m$ . Coloured circles represent the three different IDE widths and the black bars represent standard deviation. IDEs with gap  $300\mu m$  were selected to check consistency of prints, as they were present on far left, right and centre positions of a print.

Graphs represent height (Figure 39(a)) and width (Figure 39(b)) of  $200\mu m$ ,  $300\mu m$  and  $400\mu m$  width IDEs. The analysis was a collection of data from 5 different prints (4 IDEs on each print) for each plate group. Heights of the IDEs (Figure 39 (a)) positioned on the centre and end parts on a print are similar, but the ones positioned at the start of a print are higher in height compared to centre and end parts due to the silver ink drying in the anilox. Similarly the width (Figure 39(b)) of the IDEs positioned on the end part of a print are higher compared to the IDEs on start and centre positions due to the silver ink drying on the flexo plate as the print progress.

Figure 40 displays the average difference in height (figure 40(a)) and width (Figure 40(b)) of the IDEs with  $200\mu m$  width and  $300\mu m$  gap. Each blue point is an average of 3 IDEs (1 print run). Standard deviation is 0.037 in height and 8.401 in width of the IDEs which indicates the constant drying occurrence of the silver ink. The average cross-sectional area for 15 silver IDEs was  $214.2\mu m^2$  with a standard deviation of 5.09.

Only few runs were possible to print due to silver ink drying on the anilox, after which the set-up had to be cleaned. One of the limitations of RK Flexiproofer is that when the anilox is engaged, the print tends to have more ink at the start of the print when it first meets the substrate compared to the end part of the print where it is not continuously wetted.

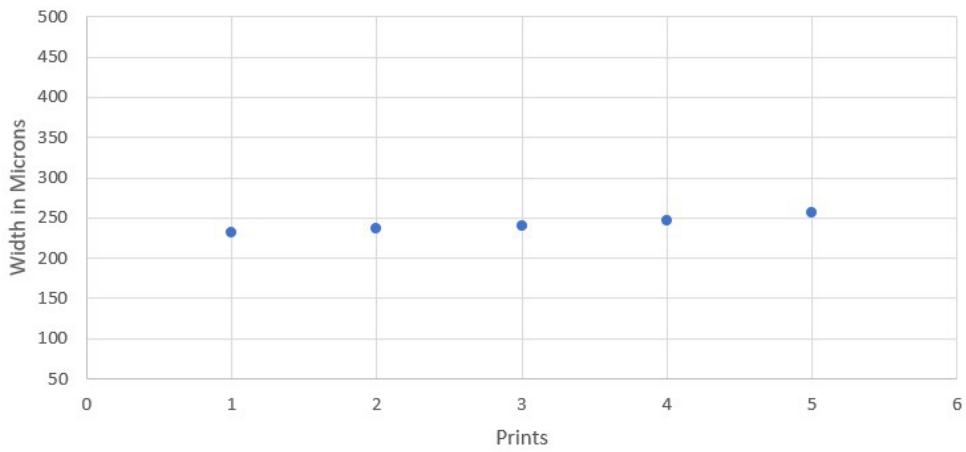
Silver IDE Height Average (200 Micron Width-300 Micron Gap IDE)



Standard Deviation	0.037
Each point is an average of 3 IDEs	

(a) Average Height

Silver IDE Track Width Average (200 Micron Width-300 Micron Gap IDE)



Standard Deviation	8.401
Each point is an average of 3 IDEs	

(b) Average Width

Figure 40: Average height and width of 200 $\mu$ m IDEs

## 4.6 Electrical Resistance of the Printed Silver IDEs

Printed Silver Interdigitated Electrodes (IDEs) were tested for their resistance using 2-point measuring method (Figure 41) on a probe station with a Keithley Digital Multimeter. Initial testing displayed that the unit of resistance was in  $\Omega$ , which is sufficient when compared to 4-point measurement method which is useful if the unit of measurement is in  $m\Omega$  or  $\mu\Omega$ . Internal resistance of the multi-meter was record at  $0.127\Omega$ . One point was connected to one of the top corners while the second one connects to the other far end of the same IDE finger.

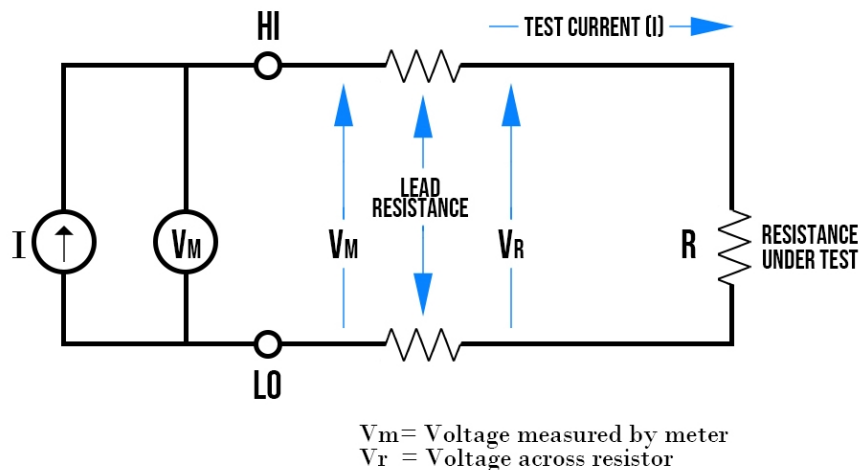


Figure 41: 2 Wire Method

Average resistance was calculated from the left and right fingers of an IDE. The resistance pattern for the IDEs with the track widths  $200$ ,  $300$  and  $40\mu m$  are shown in Figure 42. The difference in the resistance range between the three widths is due to the increasing thickness between them. The average resistance of cumulative 228 IDEs was  $11.96\Omega$  with a standard deviation of 1.21, which shows that Silver Interdigitated Electrodes (IDEs) with three different track widths show similar electrical resistivity and were consistent in the print quality. The difference in resistance across the multiple IDEs with different width and gap were also negligible (table 7).

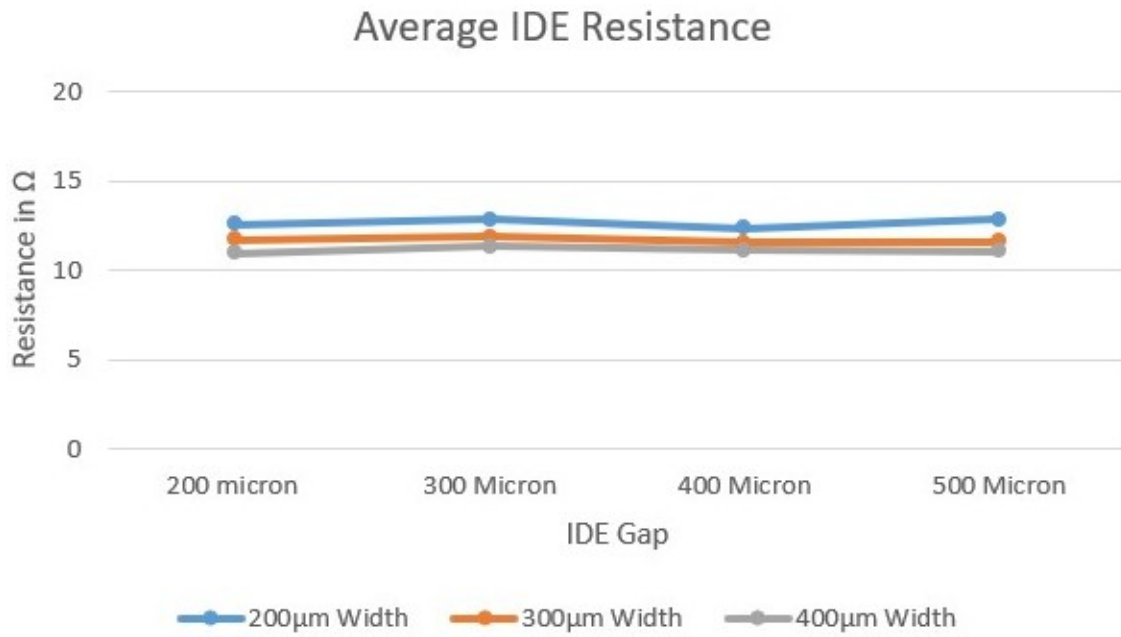


Figure 42: Average Silver IDE Resistance

Table 7: Mean Electrical Resistance of IDEs

Width of Track	Mean in $\Omega$	Standard Deviation
$200\mu m$	12.63	0.97
$300\mu m$	12.24	0.79
$400\mu m$	11.12	1.88



## 5 Humidity Chamber Testing

### 5.1 Humidity Chamber Setup

The Nafion coated interdigitated electrodes were placed inside a Sanyo MTH-2400 humidity chamber and a Keithley multimeter connected to the two ends of the fingers on the interdigitated electrodes (figure 43). The humidity chamber has the capability to operate at relative humidity ranging from 20% to 95%. The temperature for all the tests in the humidity chamber was at 25°C.

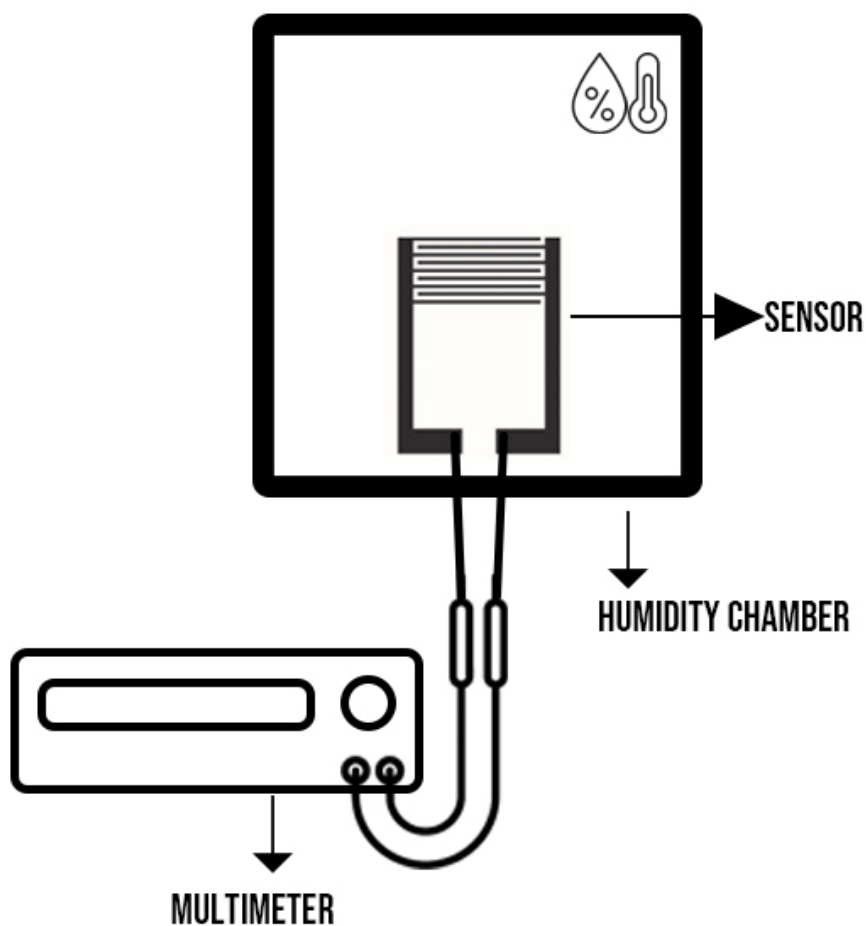


Figure 43: Relative humidity testing setup

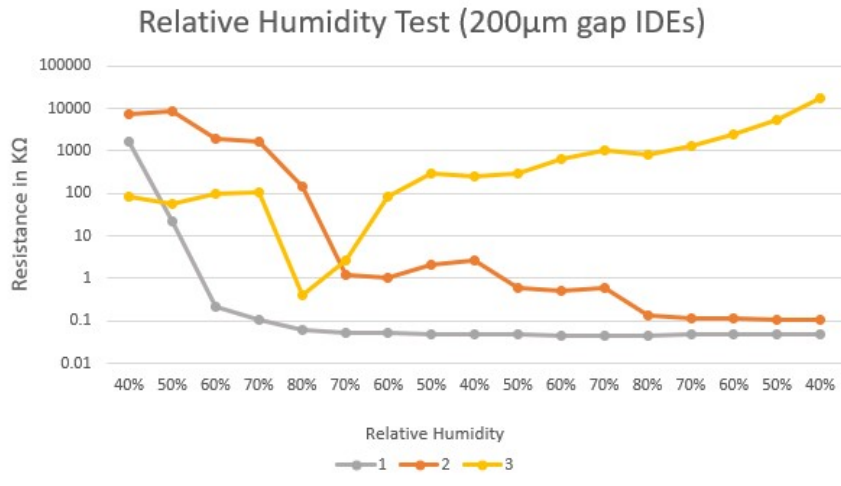
## 5.2 Direct Current measurement

Direct current was the preferred method to test the sensors as it is relatively lower in cost and easy to operate when compared to alternating current testing devices.

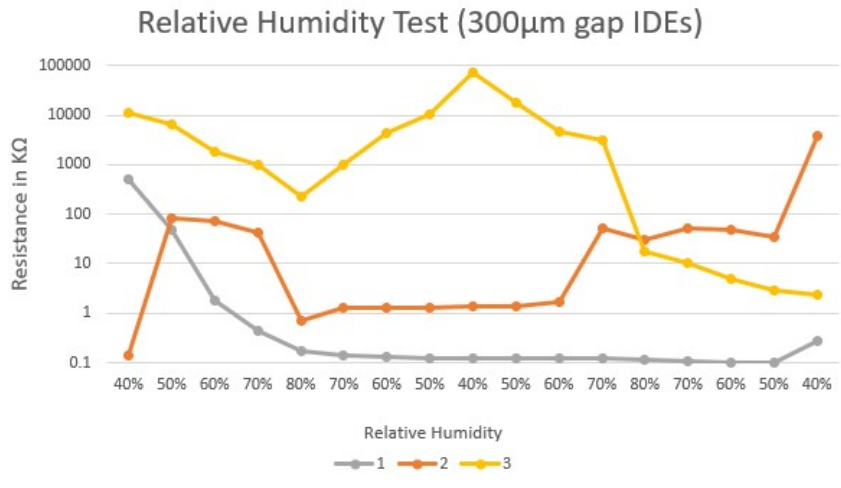
The Interdigitated electrodes were subjected to humidity ranges from 40%, 50%, 60%, 70% and 80% at 20 minutes on each range. The sensors were cycled twice from 40% to 80% and back to 40%. The first set of measurements were recorded through Keithley Multimeter with an applied voltage of 1V for the Interdigitated Electrode's (IDE) resistance. The range of resistance for the first set of IDEs tested were of 400 $\mu$ m track width and gaps from 200,300,400 and 500 $\mu$ m.

Figure 44 represents the electrical response of 200,300,400 and 500 $\mu$ m gap sensors to the change in relative humidity. All the sensors tested in DC had a fixed width of 400 $\mu$ m. Sensors with the gaps 400 $\mu$ m and 500 $\mu$ m (figure 44 [c]) lasted the longest when compared to the other gaps during the two cycles. The resistance values decrease with the increase in relative humidity as observed in Figure 44c yellow line [500 $\mu$ m sensor] where the resistance decrease to 1000 K $\Omega$  at 80% humidity and raises back to around 11000 K $\Omega$  at 40% humidity, which indicates that the Nafion exhibited expected response when subjected to humidity. Gaps smaller than 400 $\mu$ m such as sensors 1 from both 300 $\mu$ m and 200 $\mu$ m (figure 44 [a, b]) short circuited at the initial stage and remaining sensors displayed erratic response when subjected to humidity. Upon closer inspection after 2 cycles, all the sensors displayed a change in physical appearance, with a black layer forming on top of the surface which would connect the fingers of the IDEs, which decreased the performance with time. This is a black dendritic growth present on all sensors following two cycles (figure 45)

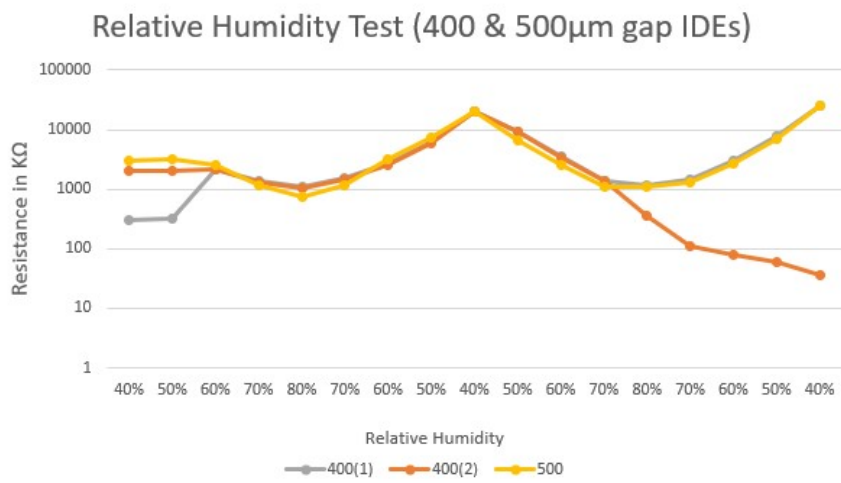
Different sensors displayed different structure formation of dendrites during 2 cycles. In figure 45 [a, b, c] due to the smaller gap, the dendrite structure was prominent on the fingers of the sensors. The sensors that were subjected to 2 full cycles (Figure 45 (a, b, c, d, e)) had the dendritic growth connecting the fingers which led to shorting of the sensors. Sensors subjected to partial cycle test (Figure 45 (e, g)) also displayed the growth of dendrites but at a smaller level. These sensors were discarded as the growth of the dendrites hindered the performance of the sensors which ultimately led them to failure at early stages.



(a) 200 $\mu$ m Gap

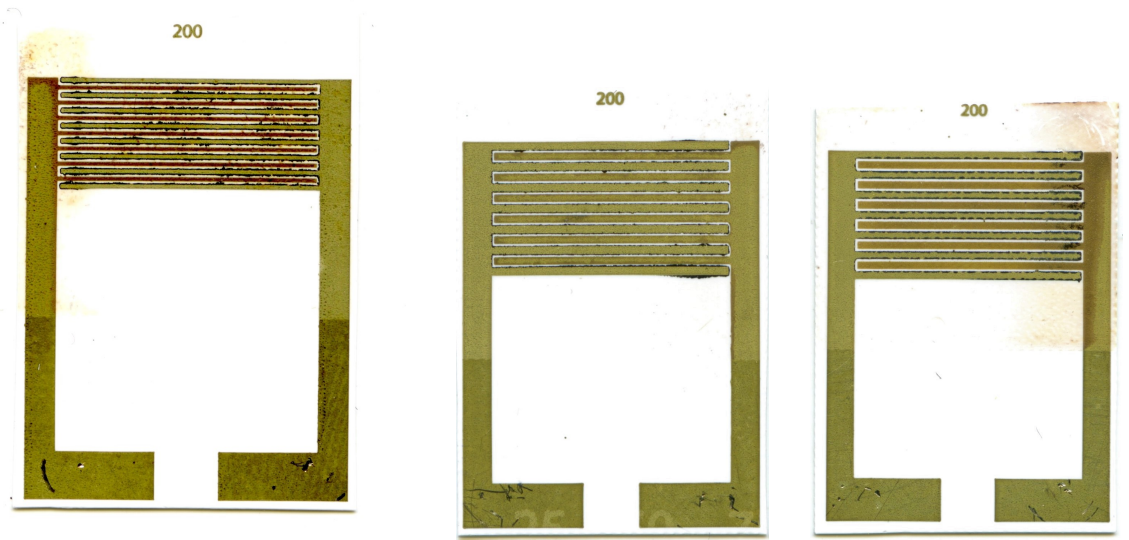


(b) 300 $\mu$ m Gap

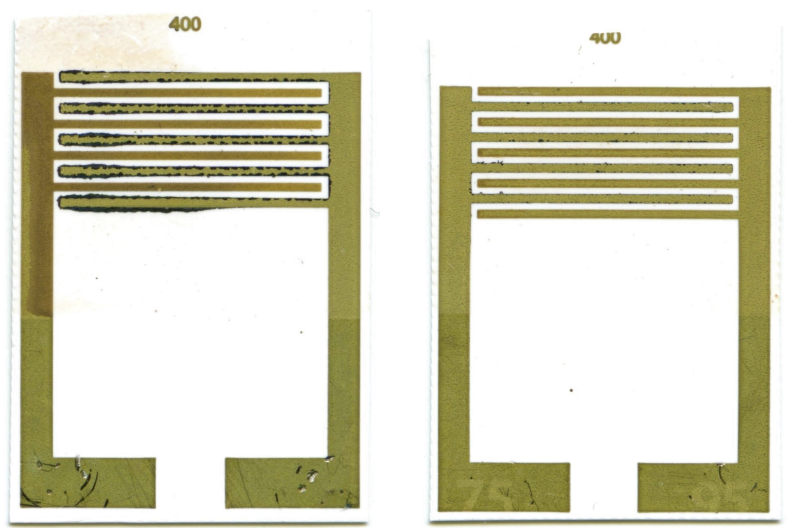


(c) 400 $\mu$ m and 500 $\mu$ m Gap

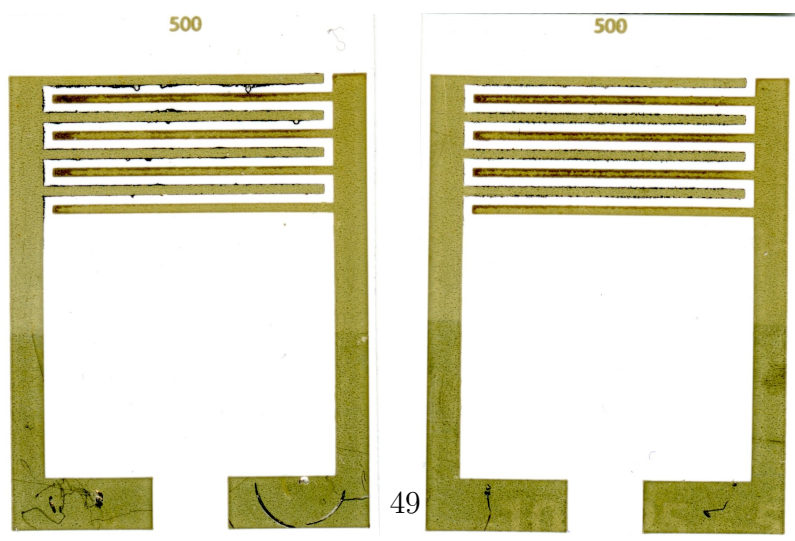
Figure 44: Electrical Resistance of 400 $\mu$ m width nafion coated IDEs



(a) 200µm Width, 200µm Gap IDE      (b) 200µm Width, 200µm Gap IDE      (c) 200µm Width, 200µm Gap IDE



(d) Particle formation after full test      (e) Particle formation after partial test



(f) 300µm Width, 500µm Gap IDE      (g) 300µm Width, 500µm Gap IDE (partial test)

Figure 45: Dendrite formation

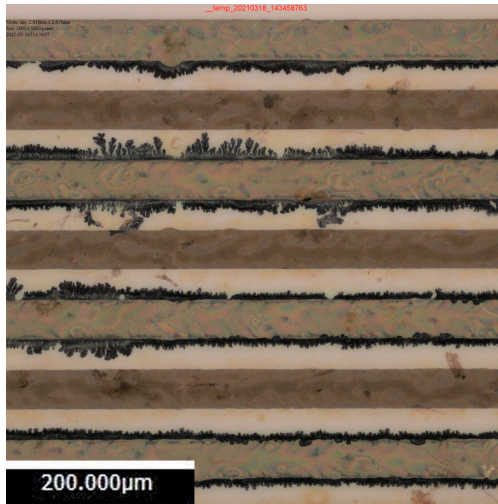
### 5.3 Dendritic Growth

The black multi-branching leaf-like structure observed on the sensor are known as Dendrites or Metal whiskering, McAllister, et al [43]. This growth of leaf-like structure is observed on elemental metals but also with alloys. This event can be triggered by different mechanical stress but particularly by residual stress caused by electroplating, which might be the cause in this situation.

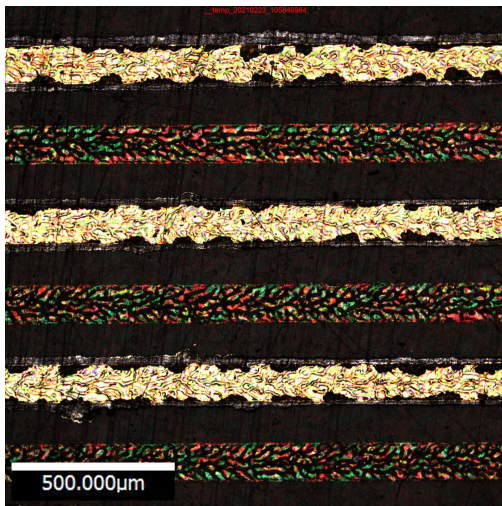
Reduction of cations of a metal by introducing direct electric current is known as Electroplating. One of the industrial practices on silver is to achieve oxidation of anions on a substrate or another metal, for example the formation of silver chloride on a silver wire to produce silver electrodes. Nafion which is used as an active layer on the sensor in this scenario was acting as a conductive bath (electrolyte) which caused a chemical reaction leading to the formation of Dendrites, the black layer of oxides that formed on the surface of a metal while passing direct current. The level of voltage and the way which direct current has one directional flow of electricity, lead to the formation of these dendrites.

Dendritic growth on a sensor when observed from a microscope (Figure 46(a) [without focused light] and Figure 46(c, d) [with focused light]) of 5x magnification displays the growth of dendrites in a branched leaf like structure. When these sensors were observed on a white light interferometer (WLI) (Figure 46(b)), it displayed the growth of dendrites on the positive finger side of the Silver Interdigitated Electrode (IDE) which is a sign of electroplating, where the positively charged finger of the IDE acts as anode and the negatively charged finger acts as cathode.

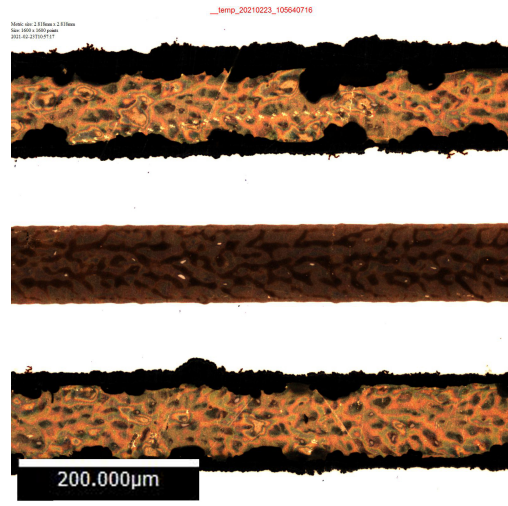
Direct current testing was paused as the sensors no longer performed as intended. Next test method was done by using alternating current which periodically changes magnitude and direction while able to push lower Voltage via LCR (Inductance, Capacitance and Resistance circuit) bridge.



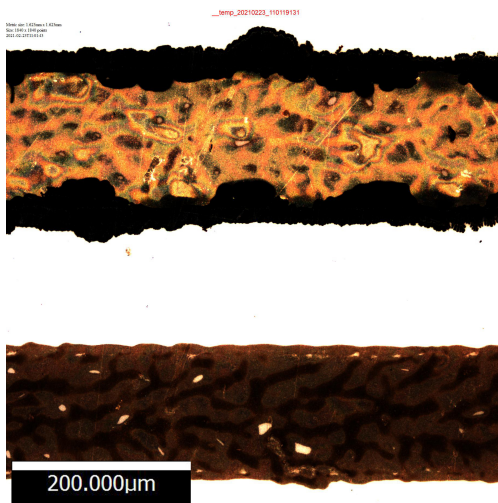
(a) 5x magnification (Width:  $200\mu m$ , Gap:  $200\mu m$ ) (Microscope)



(b) 2.5x magnification (Width:  $400\mu m$ , Gap:  $500\mu m$ ) (WLI)



(c) 5x magnification (Width:  $400\mu m$ , Gap:  $500\mu m$ ) (Microscope)



(d) 10x magnification (Width:  $400\mu m$ , Gap:  $500\mu m$ ) (Microscope)

Figure 46: Dendrite observed via microscope

## 5.4 Alternating Current measurement

Another set of Nafion coated IDEs were placed inside the environmental chamber and were tested with Alternating Current (AC) (Figure 47) using Rohde and Schwarz programmable LCR bridge meter. The resistance of the interdigitated electrodes (IDE) was recorded in serial setting (Table 8).

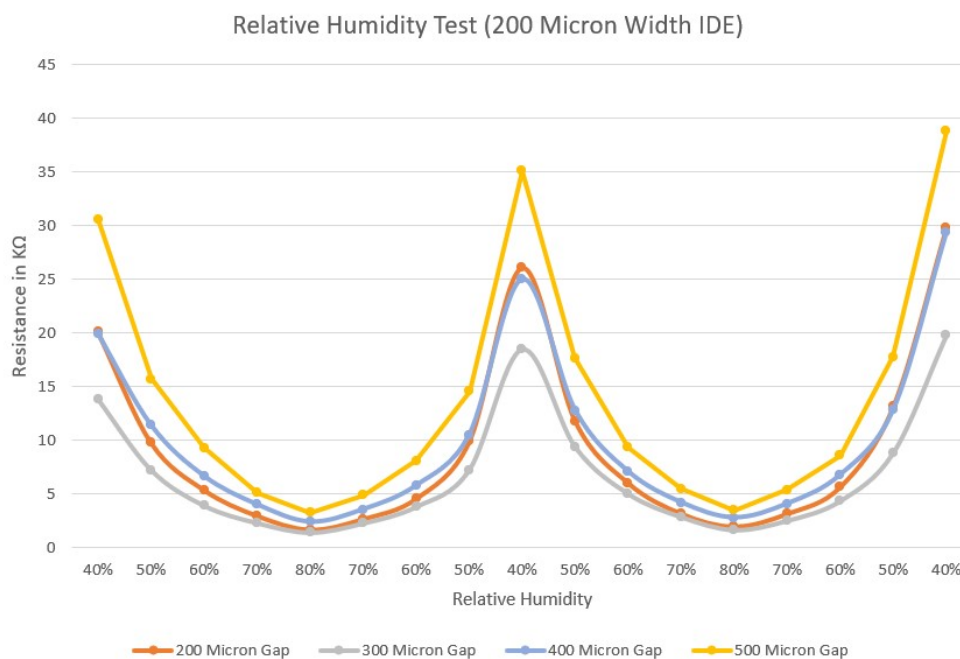
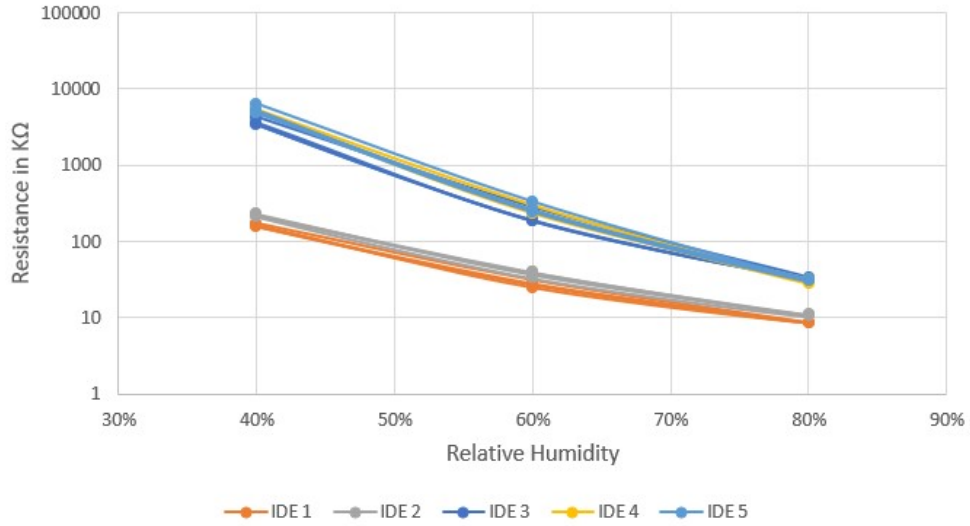


Figure 47: 200 $\mu m$  width IDE resistance tested using AC

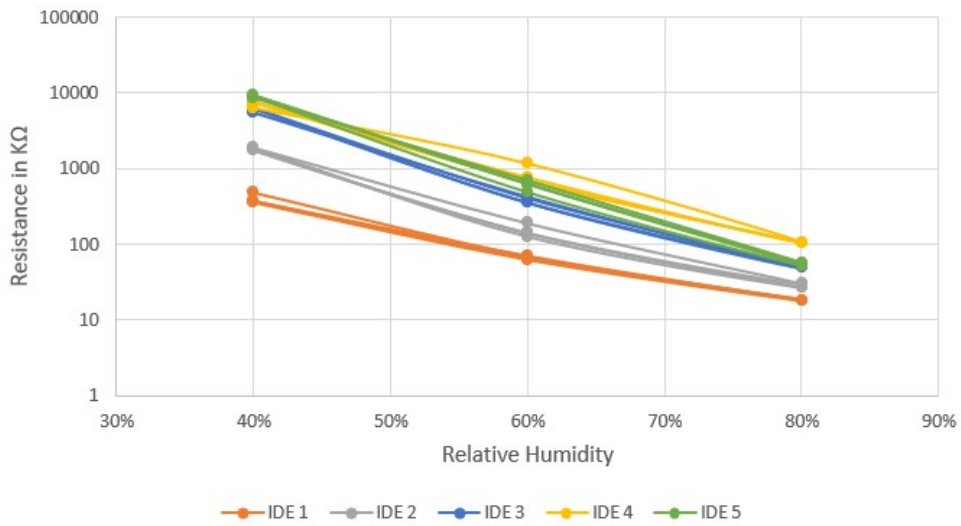
X axis represents the relative humidity of 2 cycles ranging from 40% to 80%. When the sensors were subjected to AC test with the settings as shown in Table 8, during the two cycles it displayed the potential of Nafion as an active layer, where the resistance decreased as the level of humidity increased and vice versa. Sensors with the gap 500 $\mu m$  displayed the highest variation of resistance across the various humidity ranges when compared to the smaller gaps. The resistance pattern for the Interdigitated Electrodes (IDEs) of gaps 500, 400, 300, 200 $\mu m$  have a common trend with no inconsistencies during the 2 test cycles. The range of resistance was between highs of 38.8K $\Omega$  and lows of 1.42K $\Omega$ . Another set of different IDEs of same width and same gap were tested for their range of resistance (figure 48).

Relative Humidity Test (200 Micron Width-400 Micron Gap IDE)



(a) 200μm Width

Relative Humidity Test (400 Micron Width-400 Micron Gap IDE)



(b) 400μm Width

Figure 48: Range of resistance when tested with AC



Same testing method was applied to the other new set of IDEs. Sensors (figure 48) displayed the same pattern of resistance when compared to the first set of sensors (figure 47) where the pattern of resistance was consistent, but the range at which these sensors performed was different between the different set of sensors tested, where some sensors are found to show resistance of  $600\text{ K}\Omega$  and some around  $9000\text{ k}\Omega$  at 40% humidity. (figure 47 and 48(a, b)).

Prior printing Nafion on top of silver electrode, the base silver IDE structure showed constant electrical resistance through the fingers regardless of the gaps. There are two reasons why the electrode might not be performing as expected, the silver ink used might be re-wetting during the humidity test. The second reason might be due to the electro-chemical reaction from the unique properties of Nafion layer on the sensor.

Table 8: Alternating Current Test Settings

Device	Rohde and Schwarz hm8118 LCR meter
Resistance Measured at	1KHz
Measurement Mode	Parallel
Bias Voltage	<1.3 Volts

## 5.5 Discussion

The research has shown the potential to print interdigitated electrodes by Flexography as a precursor to the development of sensors. All the 228 base printed silver Interdigitated electrodes of different gap and track width, without the Nafion were able to maintain an average resistance of  $11.96\Omega$  with a standard deviation of 1.21 which represents the print consistency. The silver even though it poses a level of difficulty to print via flexography, it can produce good and consistent results of resistance upon testing. Later when Nafion was coated on top of the silver interdigitated electrodes and tested via Direct Current (DC) at 1V, the performance of these sensors decreased rapidly and failed at an early stage due to short-circuits.

When these Nafion coated interdigitated electrodes were tested via alternating current (AC), they were able to display change in resistance according to the change in relative humidity(rH). Another inconsistency was noted where even though the sensors with the same dimensions displayed the change in resistivity, they were not equal in range. When a drop of Nafion was placed on the fingers of the silver interdigitated electrode with the help of a pipette, to make a layer thicker than the one printed via Flexographic method, the sensor showed tiny growths of dendrite formation even with Alternating Current (AC) testing method, which shows that presence of Nafion influenced the growth of dendrites.

## 6 Conclusion and Futurework

**Conclusion:** The viability of a flexographic printed humidity sensor based on an interdigitated silver electrode with a Nafion coating has been demonstrated. This could be volume produced on a label press or integrated with package production and be the basis for sensors for a wide range of applications by using alternative sensing materials. The interdigitated electrodes have been optimized in terms of gap and finger width where the finger gaps and widths from 200 to 500 $\mu m$  had similar resistance values as seen in Table 7. A minimum gap was required to avoid short circuits which was 200 $\mu m$ , where most of the IDEs with a gap of 100 $\mu m$  between the fingers were shorted and caused the sensors to fail.

Dendrite formation was observed on the sensors which were placed inside the humidity chamber and tested with Direct current (DC) and Alternating Current (AC) which caused the sensors to fail as the dendrites formed bridges connecting the fingers and shorting them as seen in Figure 46(a). Sensors that were tested with Alternating Current (AC) were self-consistent and repeatable for 2 cycles when compared to the ones tested with Direct Current (DC) which displayed erratic response in resistivity (Figure 44). Formation of dendrites was observed in the research work surrounding the development of Lithium-Ion batteries [44].

Using an alternative active material to sense the change in humidity is suggested as Nafion proved to be a difficult material to use for this specific method of application. Metal oxides such as [22–24] or other polymer based active inks such as polyaniline [30] can be tested for this application.

**Future Work:** Current work can be investigated for further research to improve the life of the sensors tested via Alternating Current (AC) by investigating the cause of dendrites, which might also reduce the cause of sensor-to-sensor variation. Presence of Sulphur in the Nafion might also be one of the reasons for the growth of dendrites,” The sulphur species influenced significantly the growth rate of Cu<sub>2</sub>S dendrites” [45]. Possible suppression of dendrites can be researched by adding supporting compounds such as Titanium Dioxide [16] to increase the sensor’s stability. Work on the development of batteries has also observed the growth of these dendrites, where there are viable solutions to suppress them as seen in [46]. Elimination of dendrites can be studied by changing the choice of using Nafion to alternative functional materials.

Even though there are challenges to develop sensors via flexographic technique, it does show the potential, but the inks that are to be used should be evaluated before presenting it as a finished device. There are also other conductive inks (gold [18], graphite [46]) and active layers (Metal oxides [22–24], polyaniline [30]) that are widely researched, where they can be incorporated into this existing interdigitated electrode design and flexographic printing technique to develop sensors with wide scope of applications.

## References

- [1] Z. Chen and C. Lu, “Humidity sensors: a review of materials and mechanisms,” *Sensor letters*, vol. 3, no. 4, pp. 274–295, 2005.
- [2] H. N. Kim, W. X. Ren, J. S. Kim, and J. Yoon, “Fluorescent and colorimetric sensors for detection of lead, cadmium, and mercury ions,” *Chemical Society Reviews*, vol. 41, no. 8, pp. 3210–3244, 2012.
- [3] Q. Lin, Q. Zhao, and B. Lev, “Cold chain transportation decision in the vaccine supply chain,” *European Journal of Operational Research*, vol. 283, no. 1, pp. 182–195, 2020.
- [4] S. Grimnes and O. G. Martinsen, *Bioimpedance and bioelectricity basics*. Academic press, 2011.
- [5] A. Rivadeneyra, J. Fernández-Salmerón, J. Banqueri, J. A. López-Villanueva, L. F. Capitan-Vallvey, and A. J. Palma, “A novel electrode structure compared with interdigitated electrodes as capacitive sensor,” *Sensors and Actuators B: Chemical*, vol. 204, pp. 552–560, 2014.
- [6] K. Suganuma, *Introduction to printed electronics*, vol. 74. Springer Science & Business Media, 2014.
- [7] A. Kamyshny and S. Magdassi, “Conductive nanomaterials for printed electronics,” *Small*, vol. 10, no. 17, pp. 3515–3535, 2014.
- [8] J. Izdebska-Podsiadły and S. Thomas, *Printing on polymers: fundamentals and applications*. William Andrew, 2015.
- [9] M. Yusof, A. A. Zaidib, T. Claypole, and D. Gethin, “The effects of anilox roller on fine line printing in flexographic printing process,” *PRINTING F U T U R E DAYS 2007*, vol. 2007, p. 211, 2007.
- [10] J. J. Licari, *Hybrid microcircuit technology handbook: materials, processes, design, testing and production*. Elsevier, 1998.
- [11] C. Hawkyard and A. Miah, “The parameters of rotary-screen printing,” *Journal of the Society of Dyers and Colourists*, vol. 103, no. 1, pp. 27–31, 1987.
- [12] D. E. Packham, “Surface energy, surface topography and adhesion,” *International journal of adhesion and adhesives*, vol. 23, no. 6, pp. 437–448, 2003.

- [13] D. Barmpakos, A. Segkos, C. Tsamis, and G. Kaltsas, “A disposable inkjet-printed humidity and temperature sensor fabricated on paper,” in *Multidisciplinary Digital Publishing Institute Proceedings*, vol. 2, p. 977, 2018.
- [14] M. Mraović, T. Muck, M. Pivar, J. Trontelj, and A. Pleteršek, “Humidity sensors printed on recycled paper and cardboard,” *Sensors*, vol. 14, no. 8, pp. 13628–13643, 2014.
- [15] B. Clifford, D. Beynon, C. Phillips, and D. Deganello, “Printed-sensor-on-chip devices— aerosol jet deposition of thin film relative humidity sensors onto packaged integrated circuits,” *Sensors and Actuators B: Chemical*, vol. 255, pp. 1031–1038, 2018.
- [16] F.-R. Hsiao and Y.-C. Liao, “Printed micro-sensors for simultaneous temperature and humidity detection,” *IEEE Sensors Journal*, vol. 18, no. 16, pp. 6788–6793, 2018.
- [17] D. Z. Vasiljević, A. Mansouri, L. Anzi, R. Sordan, and G. M. Stojanović, “Performance analysis of flexible ink-jet printed humidity sensors based on graphene oxide,” *IEEE Sensors Journal*, vol. 18, no. 11, pp. 4378–4383, 2018.
- [18] C. Sapsanis, U. Buttner, H. Omran, Y. Belmabkhout, O. Shekhah, M. Eddaoudi, and K. N. Salama, “A nafion coated capacitive humidity sensor on a flexible pet substrate,” in *2016 IEEE 59th International Midwest Symposium on Circuits and Systems (MWSCAS)*, pp. 1–4, IEEE, 2016.
- [19] J. S. Santos, I. M. Raimundo Jr, C. M. Cordeiro, C. R. Biazoli, C. A. Gouveia, and P. A. Jorge, “Characterisation of a nafion film by optical fibre fabry–perot interferometry for humidity sensing,” *Sensors and Actuators B: Chemical*, vol. 196, pp. 99–105, 2014.
- [20] C. Kutzner, R. Lucklum, R. Torah, S. Beeby, and J. Tudor, “Novel screen printed humidity sensor on textiles for smart textile applications,” in *2013 Transducers & Eurosenors XXVII: The 17th International Conference on Solid-State Sensors, Actuators and Microsystems (TRANSDUCERS & EUROSENSORS XXVII)*, pp. 282–285, IEEE, 2013.
- [21] Y. Wang, J. Wang, M. Hao, B. Li, Z. Zhu, X. Gou, and L. Li, “Rapid preparation of a nafion/ag nw composite film and its humidity sensing effect,” *RSC Advances*, vol. 10, no. 46, pp. 27447–27455, 2020.
- [22] A. Ismail, M. Mamat, M. Yusoff, M. Malek, A. Zoolfakar, R. Rani, A. Suriani, A. Mohamed, M. Ahmad, and M. Rusop, “Enhanced humidity sensing performance

- using sn-doped zno nanorod array/sno2 nanowire heteronetwork fabricated via two-step solution immersion,” *Materials Letters*, vol. 210, pp. 258–262, 2018.
- [23] B. Yadav, R. Srivastava, and C. Dwivedi, “Synthesis and characterization of zno-tio2 nanocomposite and its application as a humidity sensor,” *Philosophical magazine*, vol. 88, no. 7, pp. 1113–1124, 2008.
- [24] F. Hernandez-Ramirez, A. Tarancón, O. Casals, J. Arbiol, A. Romano-Rodriguez, and J. Morante, “High response and stability in co and humidity measures using a single sno2 nanowire,” *Sensors and Actuators B: Chemical*, vol. 121, no. 1, pp. 3–17, 2007.
- [25] W. Ahmad, M. Mamat, A. Zoolfakar, Z. Khusaimi, M. Yusoff, A. Ismail, S. Roslan, and M. Rusop, “The performance of humidity sensor using iron oxide as the sensor element,” in *2018 8th IEEE International Conference on Control System, Computing and Engineering (ICCSCE)*, pp. 217–222, IEEE, 2018.
- [26] P. He, J. Brent, H. Ding, J. Yang, D. Lewis, P. O’Brien, and B. Derby, “Fully printed high performance humidity sensors based on two-dimensional materials,” *Nanoscale*, vol. 10, no. 12, pp. 5599–5606, 2018.
- [27] H. Bi, K. Yin, X. Xie, J. Ji, S. Wan, L. Sun, M. Terrones, and M. S. Dresselhaus, “Ultra-high humidity sensitivity of graphene oxide,” *Scientific reports*, vol. 3, no. 1, pp. 1–7, 2013.
- [28] W. Lövenich, “Pedot-properties and applications,” *Polymer Science Series C*, vol. 56, no. 1, pp. 135–143, 2014.
- [29] R. M. Morais, M. dos Santos Klem, G. L. Nogueira, T. C. Gomes, and N. Alves, “Low cost humidity sensor based on pani/pedot: Pss printed on paper,” *IEEE Sensors Journal*, vol. 18, no. 7, pp. 2647–2651, 2018.
- [30] A. G. MacDiarmid and A. J. Epstein, “Polyanilines: a novel class of conducting polymers,” *Faraday Discussions of the Chemical Society*, vol. 88, pp. 317–332, 1989.
- [31] C. Nash, Y. Spiesschaert, G. Amarandei, Z. Stoeva, R. I. Tomov, D. Tonchev, I. Van Driessche, and B. A. Glowacki, “A comparative study on the conductive properties of coated and printed silver layers on a paper substrate,” *Journal of Electronic Materials*, vol. 44, no. 1, pp. 497–510, 2015.

- [32] J. C. Wyant, “White light interferometry,” in *Holography: A Tribute to Yuri Denisyuk and Emmett Leith*, vol. 4737, pp. 98–107, International Society for Optics and Photonics, 2002.
- [33] H. A. Barnes, J. F. Hutton, and K. Walters, *An introduction to rheology*, vol. 3. Elsevier, 1989.
- [34] S. Emamian, B. B. Narakathu, A. A. Chlaihawi, B. J. Bazuin, and M. Z. Atashbar, “Screen printing of flexible piezoelectric based device on polyethylene terephthalate (pet) and paper for touch and force sensing applications,” *Sensors and Actuators A: Physical*, vol. 263, pp. 639–647, 2017.
- [35] H. Karian, *Handbook of polypropylene and polypropylene composites, revised and expanded*. CRC press, 2003.
- [36] S. Jabarin and E. Lofgren, “Thermal stability of polyethylene terephthalate,” *Polymer Engineering & Science*, vol. 24, no. 13, pp. 1056–1063, 1984.
- [37] M. Rebros, P. D. Fleming, and M. K. Joyce, “Uv-inks, substrates and wetting,” in *Proceedings of the 2006 TAPPI Coating & Graphic Arts Conference, Atlanta*, Citeseer, 2006.
- [38] R. J. Young and P. A. Lovell, *Introduction to polymers*. CRC press, 2011.
- [39] D. W. Hatchett and M. Josowicz, “Composites of intrinsically conducting polymers as sensing nanomaterials,” *Chemical reviews*, vol. 108, no. 2, pp. 746–769, 2008.
- [40] K. A. Mauritz and R. B. Moore, “State of understanding of nafion,” *Chemical reviews*, vol. 104, no. 10, pp. 4535–4586, 2004.
- [41] X. Liu, J. Guthrie, and C. Bryant, “A study of the processing of flexographic solid-sheet photopolymer printing plates,” *Surface Coatings International Part B: Coatings Transactions*, vol. 85, no. 4, pp. 313–319, 2002.
- [42] M. Vakilian and B. Y. Majlis, “Study of interdigitated electrode sensor for lab-on-chip applications,” in *2014 IEEE International Conference on Semiconductor Electronics (ICSE2014)*, pp. 201–204, IEEE, 2014.
- [43] A. K. McAllister, “Cellular and molecular mechanisms of dendrite growth,” *Cerebral cortex*, vol. 10, no. 10, pp. 963–973, 2000.



- [44] F. Han, A. S. Westover, J. Yue, X. Fan, F. Wang, M. Chi, D. N. Leonard, N. J. Dudney, H. Wang, and C. Wang, “High electronic conductivity as the origin of lithium dendrite formation within solid electrolytes,” *Nature Energy*, vol. 4, no. 3, pp. 187–196, 2019.
- [45] Q. Han, S. Sun, J. Li, and X. Wang, “Growth of copper sulfide dendrites and nanowires from elemental sulfur on tem cu grids under ambient conditions,” *Nanotechnology*, vol. 22, no. 15, p. 155607, 2011.
- [46] M. K. Aslam, Y. Niu, T. Hussain, H. Tabassum, W. Tang, M. Xu, and R. Ahuja, “How to avoid dendrite formation in metal batteries: innovative strategies for dendrite suppression,” *Nano Energy*, vol. 86, p. 106142, 2021.
- [47] [https://www.alicon.com/fileadmin/\\_processed\\_/d/7/csm\\_VFP\\_rund\\_schattiert\\_06f5a4c92e.png](https://www.alicon.com/fileadmin/_processed_/d/7/csm_VFP_rund_schattiert_06f5a4c92e.png) (11/10/2021).